T2R2 東京科学大学 リサーチリポジトリ
Science Tokyo Research Repository

論文 / 著書情報
Article / Book Information

題目(和文)	分子幾何構造の利用による典型的な芳香族炭化水素の蛍光機能化
Title(English)	Molecular-Geometry Approaches to Develop Functional Fluorophores Based on Classic Aromatic Hydrocarbons
著者(和文)	佐々木俊輔
Author(English)	Shunsuke Sasaki
出典(和文)	学位:博士(工学), 学位授与機関:東京工業大学, 報告番号:甲第10579号, 授与年月日:2017年3月26日, 学位の種別:課程博士, 審査員:小西 玄一,安藤 慎治,石谷 治,腰原 伸也,川内 進
Citation(English)	Degree:Doctor (Engineering), Conferring organization: Tokyo Institute of Technology, Report number:甲第10579号, Conferred date:2017/3/26, Degree Type:Course doctor, Examiner:,,,,
学位種別(和文)	博士論文
Category(English)	Doctoral Thesis
種別(和文)	要約
Type(English)	Outline

Powered by T2R2 (Science Tokyo Research Repository)

博士論文要約

Molecular-Geometry Approaches to Develop Functional Fluorophores Based on Classic Aromatic Hydrocarbons

Shunsuke Sasaki

2017

School of Materials and Chemical Technology
Department of Chemical Science and Engineering
Tokyo Institute of Technology

General Introduction

1. Concepts of Electronic States and Their Mixing

2. Material Science Based on the Concept of TICT

3. Philosophy of this Thesis

4. Abstracts for this Thesis

5. References

1. Concepts of electronic states and their mixing

1-1. molecular orbital theory versus electronic state model: material science viewpoints

Over the decades, enormous π-conjugated organic molecules have been developed as promising materials for organic optoelectronics,[1] fluorescence imaging,[2] nonlinear optics,[3] colorimeter for subtle chemical species and other external stimuli,[4] memory devices[5] and photoredox catalysts.[6] Developments of these materials necessarily require deep understanding and precise control of their excited states as well as their ground states. For material scientists, control of molecular orbitals, especially of frontier orbitals, have been considered to be a first choice to optimize properties of designed molecules. Therefore, design of π-conjugated organic molecules have been considered to be manipulation of energy levels and spatial distributions of highest occupied molecular orbital (HOMO) and lowest unoccupied molecular orbital (LUMO). The design of HOMO and LUMO has been achieved by appropriate choice of a core chromophore and substituents. Recent developments of organic synthesis have allowed us to use novel chromophores with unusual frontier orbitals.[7]

Needless to say, such a molecular orbital approach is effective to understand electronic structure of well-defined molecular structure. However, there are several reasons why this approach cannot be regarded to be the best for designing π-conjugated molecules from scratch. First reason is the difficulty to imagine molecular orbitals. Though the processes that we can conduct in our brain are limited to Hückel or extended Hückel method (by means of group theory) with constant parameters, even qualitative discussion of molecular orbitals requires us at least to take coulomb and exchange interactions between electrons, anti-symmetry of wavefunctions and electronic correlations into accounts. Second reason is the inconsistency with photophysical properties. Although molecular orbitals given by computational methodology well describe characteristics of ground state, energy levels, spatial distribution, and chemical nature of excited states are sometimes disparate from those inferred from molecular orbitals. Taking benzene for example, first-order configuration interactions (CI) of four degenerated HOMO-LUMO transitions result in new S_1 and S_2 states whose chemical nature are completely different from original HOMO-LUMO transitions (Figure 1).[8] The same thing, CI between HOMO-1 ($2b_{1u}$) - LUMO ($2b_{2g}$) and

HOMO ($1a_u$) - LUMO+1 ($2b_{3g}$) transitions (both transitions are strongly allowed) makes one of their linear combination ($^1B_{3u}$) lower than HOMO-LUMO transition ($^1B_{2u}$) and severely forbidden.[9]

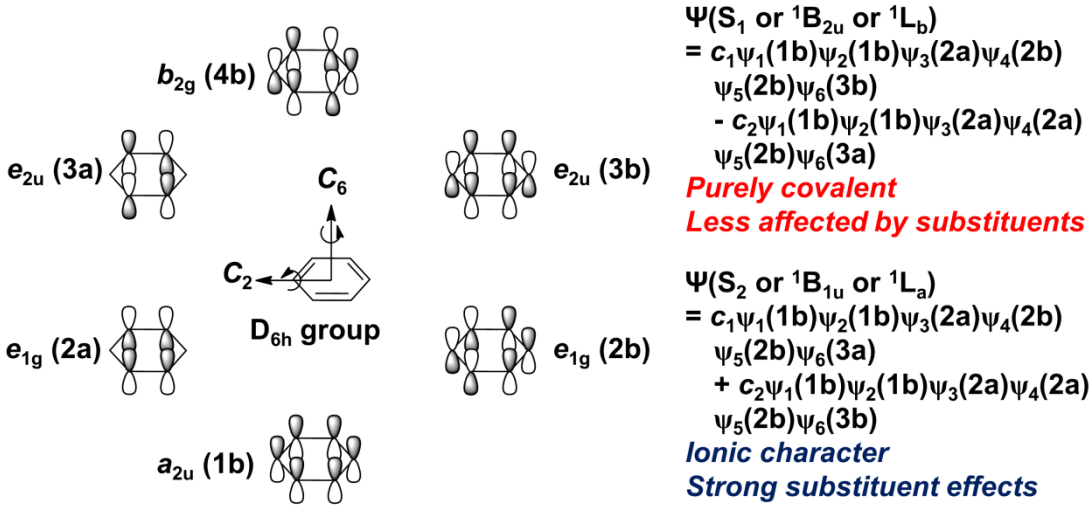

Figure 1. (left) molecular orbital of benzene labelled by D_{6h} point group (symmetry labelled by the C_2 axis in parentheses), (right) descriptions of S_1 and S_2 as linear combinations of electronic configurations.[8] c_1 and c_2 are a CI coefficient of each configuration, respectively.

The limitation of human intuition is the serious problem on the molecular design nevertheless of wide availability of modern computational techniques. To design π-conjugated molecules, one must embody abstract image of electronic structure (*e.g.* localization of frontier orbitals, ionic or covalent nature, spin-orbital interactions, potential energy surface of ground and excited states) into defined chemical structure. The sequence of ideation is not compatible with computational technique; a computer never tells us an electronic structure without inputting a well-defined chemical structure. Therefore, any framework that **directly** gives an intuitive and empirical image of an "electronic state" should be more helpful for us to design π-conjugated molecules with optimum photophysical and photochemical properties than the indirect and complicated molecular orbital approach. Following sections summarize the concise image of electronic states of polycyclic aromatic hydrocarbons (PAHs) and how they can be combined to afford blueprints of electronic structures of large and elaborated π-systems.

1-2. A free electron traveling in a one-dimensional loop and Platt's notation[12]

In parallel with the development of LCAO (linear-combination-of-atomic-orbitals) molecular orbital theory, several theoretical frameworks starting from free-electron models were postulated to interpret spectral features, diamagnetism and electric properties of molecular substances. The method assumed that the π-electrons of a planar conjugated system freely move along their bonds under a potential which was, in first approximation, constant. To enhance accuracy of the model, periodic potential was sometimes introduced just like the Bloch's periodic potential for the band theory. Despite its simplicity, the free-electron model gave better results on reproducing excitation wavelengths, oscillator strengths and polarizations of polyene,[10] porphyrin[11] and PAHs[12] than the LCAO-MO model.

Platt adopted the free-electron model with periodic potential approximation to directly obtain intuitive image of electronic states of PAHs skipping bothersome procedures of MO descriptions.[12] When a free electron is traveling in a one-dimensional loop of constant potential around the perimeter (length l), energy eigenvalues E [cm^{-1}] and eigenstate $\psi(x)$ are quantized by the periodic boundary condition $\psi(x) = \psi(l)$ as follows.

$$\psi(x) = e^{-\frac{2\pi i}{l}qx} \tag{1}$$

$$E = \frac{q^2h^2}{2ml^2} \tag{2}$$

where q is an quantum number 0, 1, 2, ⋯ that represents angular momentum and number of nodes; h is Planck's constant [erg s^{-1}]; m is the mass of the electron [g]. Under the assumption of the constant potential, the states with same quantum number q are doubly degenerated except for $q = 0$. Each of degenerated states has opposite angular momentum $+\boldsymbol{q}$ and $-\boldsymbol{q}$, respectively. Hence a PAH that consists of n ring and $2(2n+1)$ π-electrons and carbons occupies these eigenstates from $q = 0$ to $q = n$. For instance, anthracene ($n = 3$) has 14 electrons and its highest occupied state is $q = 3$. At ground state, total angular momentum $\boldsymbol{Q} = \Sigma\boldsymbol{q} = 0$ and excitation to lowest unoccupied state ($q = n + 1$) change it to $\boldsymbol{Q} = \pm 1$ or $\boldsymbol{Q} = \pm(2n + 1)$. Platt designated the states with $\boldsymbol{Q} = 0, \pm 1, \pm 2 \cdots$ by A, B, $C \cdots$ and $\boldsymbol{Q} = \pm 2n, \pm(2n + 1), \pm(2n + 2) \cdots$ by K, L, $M \cdots$. Thus, first singlet excited states were ^1B and ^1L under the constant potential approximation. Then, electron-electron interactions could be introduced empirically by Hund's rule;

triplets lied below corresponding singlets and within the group of same spin multiplicity, and states of high $|\boldsymbol{Q}|$ (e.g. ^1L state) lied below low $|\boldsymbol{Q}|$ states (e.g. ^1B state).

Herein, the periodic-potential approximation has been introduced. Figure 2 illustrates the procedure to analyze excited states of given PAHs. Due to the periodicity of potential, there are two independent set of nodes; one locates nodes at bonds ($_a$ –set) and another on atoms ($_b$ –set). An excited electron populates antinodes of the diagram and nodes indicate absence of an excited electron. Periodic potential is likely to stabilize $_a$ –set, where electrons are on atoms, more than $_b$ –set. Therefore the level of ^1L_a state get drastically lowered as the number of atoms increases while ^1L_b state is relatively insensitive to size of PAHs. As a result, S_1 is ^1L_b state for benzene, naphthalene and azulene but ^1L_a state becomes lower than ^1L_b state for anthracene, tetracene and pentacene.

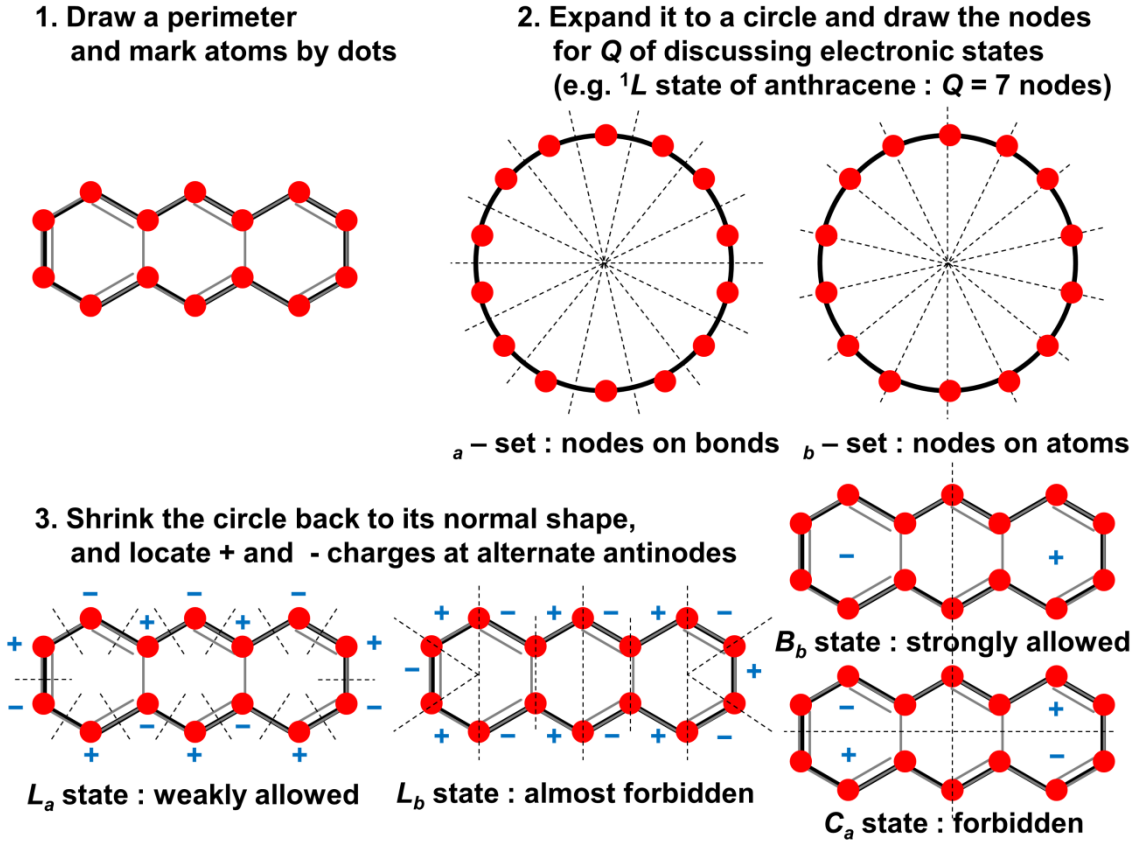

Figure 2. The procedure to classify excited states of PAHs proposed by Platt.[12]

Though + and – signals in Figure 2 do not signify partial electric charges of an excited state, the size and direction of a pseudo-electric moments calculated from these

+ and – signals will give a qualitative idea of a **transition dipole moment** (not a permanent dipole moment of an excited state). As Figure 2 indicates, ^1A–^1B transitions are strongly allowed but ^1A–^1C transitions are severely forbidden in centrally symmetric systems. ^1A–^1L transitions are multipole transitions with the odd parity, and thus their transition dipole moments (or oscillator strength *f*) are usually small. Features of each state, whose validities were confirmed by experimental results, are summarized as follows;[12]

^1L_b : S_1 of benzene, naphthalene and phenanthrene, S_2 of other larger PAHs. Its transition dipole is small and polarized along longer axis for linear PAHs (e.g. anthracene) while it is polarized along shorter axis for azulene and phenanthrene. Their molar extinction coefficients ε are around 300 – 400 [M^{-1} cm^{-1}]. Due to the absence of electrons on atoms, the level of ^1L_b state is less affected by substituents but particular substitution patterns such as 2- or 2,6- substitutions of anthracene were reported to cause mixing between ^1L_b and ^1L_a and to make ^1L_b state optically allowed.[13]

^1L_a : S_2 of benzene and naphthalene, S_1 of other larger PAHs. Its transition dipole is always perpendicular to that of ^1L_b state. Their molar extinction coefficients ε are around 5000 – 7000 [M^{-1} cm^{-1}]. Due to large electron density on atoms, ^1L_a state can be affected significantly by substituents and strongly mixed with ^{1}CT state. ^1L_b–^1L_a gap of naphthalene is 3600 cm^{-1} (experimental)[16] and thus the order of energy level can easily be inverted by introduction of strong donor or acceptor. On the other hand, ^1L_b–^1L_a gap is so wide for benzene (10500 cm^{-1}, experimental)[14-15] that substitution of even strong donor and acceptor cannot invert the order.[17-18]

^1B_b, ^1B_a : These two states are doubly degenerated in benzene corresponding to $^1A_{1g}$–$^1E_{1u}$ transition. In other PAHs they are split into lower ^1B_b and higher ^1B_a band. While intensity of a ^1A–^1B_a band remains constant regardless of the size of PAHs, intensity of a ^1A–^1B_b band smoothly increase with molecular length. It is also noteworthy that the wavelength of a ^1A–^1B_b band accords with that of polyenes of the same molecular length.

^3L_a : The phosphorescent level of typical PAHs has been assigned to ^3L_a state. ^3L_a–^1L_a gap varies smoothly with length, from 19000 cm^{-1} in benzene to 12000 cm^{-1} in

anthracene, phenanthrene and tetracene (Small singlet-triplet gap of phenanthrene is due to the existence of ^1L_b state as S_1).

1-3. Substituent effects: the symmetry-allowed mixing between ^{1}CT and ^{1}LE state

The electronic states with which the Platt's free-electron model dealt were so-called locally excited (LE) states. LE states are almost localized on PAHs and feature small change of dipole moment induced by photoexcitation ($\Delta\mu$). Even azulene, which is famous for large ground-state polarization, exhibits $\Delta\mu$ = -2.3 [D] for ^1L_b (S_1) and $\Delta\mu$ = -1.6 [D] for ^1L_a (S_2).[19] When either an electron donating group (donor or D) or an electron withdrawing group (acceptor or A) is introduced onto PAHs, there should be gradient of electric field so that photoexcitation leads charge transfer. The section describes how photophysical properties of the singlet charge transfer (^{1}CT) state can be manipulated by the mixing with ^{1}LE state.

When D and A are well separated from each other and their electronic coupling is negligibly small, there should be two excited states; one is electron-transfer (^{1}ET) state, in which single electron completely migrates from donor to acceptor, and another is ^{1}LE state of either donor or acceptor. In this case ^{1}ET and ^{1}LE state do not mix with each other and retain its own nature regardless of reaction coordinate. Slight ^{1}ET-^{1}LE mixing happens only at their intersection (**Point a** in Figure 3a), which sometimes results in S_2/S_1 conical intersection.[20] Photoexcitation initially generates ^{1}LE state and undergo non-adiabatic electron transfer reaction, whose kinetics follows Marcus theory.[21] Finally, ^{1}ET state is subject to back electron transfer reaction toward ground state in either radiative or non-radiative way. The overall process was described by the combination of Marcus theory and Fermi's golden rule.[22]

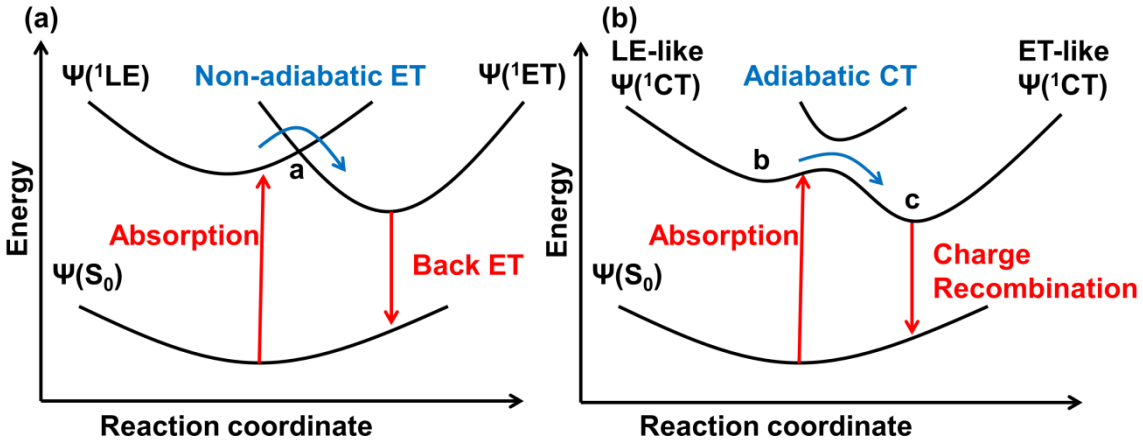

Figure 3. Potential energy surface of (a) non-adiabatic electron transfer and (b) adiabatic charge transfer reaction.

On the other hand, strong electronic coupling between a donor and an acceptor, which is seen in many substituted π-conjugated systems, combines ^{1}LE with ^{1}ET to afford ^{1}CT state over entire range of reaction coordinates. The proportions of ^{1}LE and ^{1}ET characters vary by reaction coordinates. For example, ^{1}LE character may be predominant at the **point b** of Figure 3b but strong polarization due to ^{1}ET character can be expected at the **point c**. In this case, both initial and finite states are ^{1}CT state and therefore an excited-state reaction between them should be adiabatic.[23]

Electronic-state mixing was firstly introduced by Mulliken[24] to theoretically treat molecular complex such as R_3N-BX_3, I_2-benzene and C_2H_4-Ag^+. In the case of molecular complex, the mixing happens between neutral and non-bonding state ψ(D,A) and dative state (or charge-transfer state) $\psi(D^+-A^-)$. Thus ground-state wavefunction is

$$\Psi(S_0) = g_1\psi(D,A) + g_2\psi(D^+ - A^-) \quad (3)$$

$$g_1^2 + 2g_1g_2S + g_2^2 = 1 \text{ where } S = \int \psi^*(D,A)\psi(D^+ - A^-)\,d\tau \quad (4)$$

According to second-order perturbation theory, the energy of ground state $E(S_0)$ after the electronic-state mixing is described as follows;

$$E(S_0) \approx E(D,A) - \frac{\left(\int \psi^*(D,A)\hat{H}\psi(D^+ - A^-)\,d\tau - SE(D,A)\right)^2}{E(D^+ - A^-) - E(D,A)} \quad (5)$$

$$E(D,A) = \int \psi^*(D,A)\hat{H}\psi(D,A)\,d\tau \quad (6)$$

$$E(\mathrm{D}^+ - \mathrm{A}^-) = \int \psi^*(\mathrm{D}^+ - \mathrm{A}^-)\hat{H}\psi(\mathrm{D}^+ - \mathrm{A}^-)\, d\tau \qquad (7)$$

$\hat{H}$ is the exact Hamiltonian operator for the entire set of nuclei and electrons. Both energy terms, *i.e.* E(D,A) and E(D^+−A^-) take ionic, ion-dipole, dipole-dipole, hydrogen bridge, London dispersion, exchange repulsion forces between D and A into account. Equation (5) tells us the essential requirement for electronic-state mixing; the first requirement is that **both electronic states must possess same spin multiplicity and symmetries which are non-orthogonal with each other**; the second requirement is that **the energy gap between each electronic state must be small**. These requirements can be regarded to be analogous with orbital interactions. Since the electronic-state mixing is expressed simply by the linear combination, the same treatment is applicable to various type of electronic-state mixing.

As for substituted π-conjugated systems (Figure 3b), the electronic-state mixing involves ground state (S_0), ^{1}LE state and ^{1}ET state. This three-state model has been advanced by Murrell[25] and Mulliken and Person.[26] In addition to molecular complexes,[27] this model was successfully applied to common D-π-A systems.[28] As well as Mulliken's two-state model, each wave function can be expressed by a linear combination of electronic states;

$$\Psi(\mathrm{S}_0) \approx g_1\psi(\mathrm{S}_0) + g_2\psi(\,^1\mathrm{ET}) \text{ with } g_1^2 + g_2^2 = 1 \qquad (8)$$

$$\Psi(\,^1\mathrm{CT}) \approx c_1\psi(\,^1\mathrm{ET}) + c_2\psi(\,^1\mathrm{LE}) - c_3\psi(\mathrm{S}_0) \text{ with } c_1^2 + c_2^2 + c_3^2 = 1 \qquad (9)$$

$$\Psi(\,^1\mathrm{LE}) \approx e_1\psi(\,^1\mathrm{LE}) - e_2\psi(\,^1\mathrm{ET}) \text{ with } e_1^2 + e_2^2 = 1 \qquad (10)$$

Provided that ^{1}ET−S_0 gap is far larger than ^{1}ET−^{1}LE (before mixing) gap, contribution from S_0 become negligible and these coefficients can be approximated as $c_1 \approx e_1$, $c_2 \approx e_2$, $c_3 \ll c_1, c_2$. The result demonstrates that ^{1}ET character on Ψ(^{1}LE) get stronger as ^{1}LE character increases on Ψ(^{1}CT) and in the extreme case, both Ψ(^{1}LE) and Ψ(^{1}CT) become seemingly indistinguishable can be treated equally as ^{1}CT state. Such a mixing between optically forbidden ^{1}ET state and optically allowed ^{1}LE state is called "borrowing mechanism" because oscillator strengths of S_0−^{1}CT band and S_0−^{1}LE band are sometimes inversely proportional to each other.[28] As the requirements for electronic-state mixing has instructed, also ^{1}ET−^{1}LE mixing requires each state to be closely lying and in appropriate symmetry. Empirically, ^{1}ET−^{1}LE mixing is likely to be efficient when direction of transition moment of ^{1}LE is parallel to polarization of ^{1}ET

state. Conversely, when transition moment of ^{1}LE state and polarization of ^{1}ET is in orthogonal relationship, the mixing tends to be weak.[29]

1-4. Molecular-geometry dependence of ^{1}ET-^{1}LE mixing: the concept of TICT

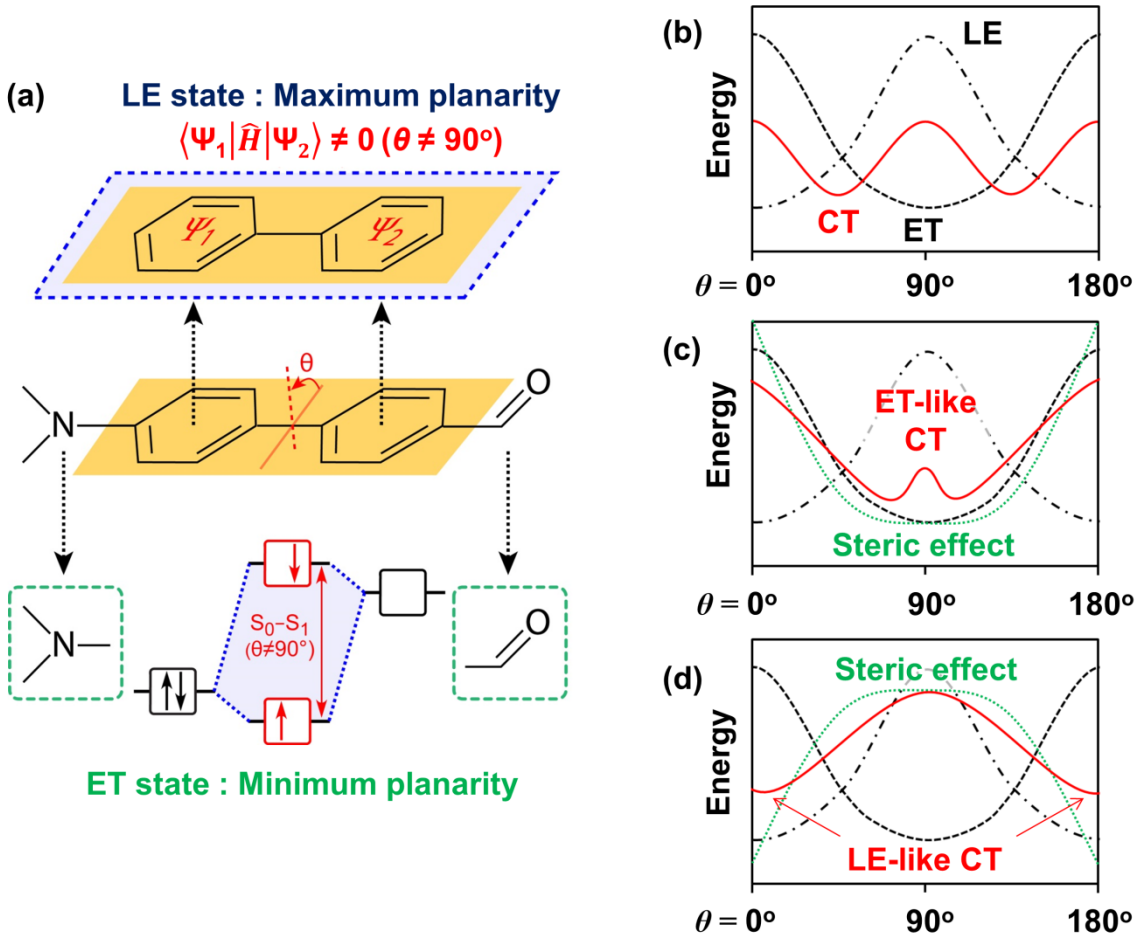

Figure 4. (a) Preferred geometries of ^{1}LE and ^{1}ET state; Schematic image of energy diagram of ^{1}LE (−·−·−), ^{1}ET (− − −) and ^{1}CT (−) states (b) when ^{1}LE character and ^{1}ET character are comparable to each other and when the steric restriction (···) is introduced (c) to twist the D-A junction (*e.g.* an alkyl group at *ortho*-position) and (d) to make the D-A junction coplanar (*e.g.* a carbon bridge).

As insisted in section 1-3, the ^{1}CT state arising from strong ^{1}ET–^{1}LE mixing changes its proportions of ^{1}ET and ^{1}LE characters continuously depending on the reaction coordinate. In addition to dielectric relaxation with a solute and solvents, torsion at D-A junction is the principal coordinate that governs the proportions of ^{1}ET and ^{1}LE characters. To control the nature of ^{1}CT state by means of molecular geometry,

it must be elucidated how ^{1}ET–^{1}LE mixing affects the equilibrium geometry of ^{1}CT state.

The seminal review about twisted intramolecular charge transfer (TICT) compiled intuitive, but insightful answer about the question and it has been employed as the essential basis for engineering ^{1}CT states of various D-π-A systems.[30] On an adiabatic energy surface of ^{1}CT state (Figure 3b), ^{1}ET and ^{1}LE states exert opposite forces to each other. The force that twists a D-A junction has ^{1}ET character whereas the force that prefers a coplanar conformation arises from mixing with a ^{1}LE state (Figure 4a). ^{1}ET state of a D-π-A system is associated with a pair of donor and acceptor orbitals[a] and consequently a perpendicular conformation minimizes the energy of ^{1}ET state. In contrast, mesomeric interaction between π-subsystems (Ψ_1 and Ψ_2) stabilizes the ^{1}LE state in a coplanar conformation.[b] These competing two forces divide the ^{1}CT surface to generate either single or multiple minima (Figure 4b). When the ^{1}ET character outweighs ^{1}LE character of ^{1}CT, the ^{1}CT minimum distinctly becomes a TICT state (Figure 4c).

The relatively simple concept that governs ^{1}ET–^{1}LE mixing opens up a myriad of possibilities for designing novel functional molecules; the competition between ^{1}LE and ^{1}ET character of ^{1}CT can easily be manipulated by adjusting several factors, including steric restrictions, polarity environments, and D-A efficacy and strength. For example, the introduction of steric hindrances such as an alkyl group at *ortho*-position of D-A junction deforms ^{1}CT surface to locate its minima at a severely twisted conformation (Figure 4c). At that conformation, ^{1}LE state is too destabilized to mix efficiently with ^{1}ET state and therefore, ^{1}CT minimum becomes highly twisted and polarized state (i.e. TICT state). On the other hand, when a steric restriction such as a carbon bridge between a donor and an acceptor forces the D-A junction to be coplanar, the ^{1}LE state is sufficiently stabilized so that ^{1}CT minimum is governed by ^{1}LE character (i.e. coplanar ICT state, Figure 4d). Polarity of surrounding environment brings about similar effect on ^{1}ET–^{1}LE mixing and such a polarity effect can be employed to design a fluorescence imaging agents.

^{1}CT potential surfaces in Figure 4b-c consist of single minima and therefore they should not exhibit dual fluorescence, even though it is often refer to as the representative phenomenon of TICT state. To generate double minima at the ^{1}CT

potential surface by positioning ^{1}ET and ^{1}LE energy diagrams appropriately, steric restriction, polarity environments, and D-A efficacy and strength must be controlled strictly. Therefore such a condition is quite limited. Nevertheless, *N*,*N*-dimethylaminobenzonitrile (DMABN) and its wide variety of analogues exhibit apparent dual fluorescence in various conditions. It is low-lying ^1L_b state of benzene what makes DMABN special among many TICT-active molecules.[18] For symmetry reason, ^{1}ET state of DMABN preferentially mixes with ^1L_a state rather than ^1L_b state[17] but ^1L_b–^1L_a gap is so large for benzene that ^1L_b state is still low-lying compared to ^1L_a – like and coplanar ICT state (Figure 5).[18] Thus, so-called LE emission of DMABN[30] is from ^1L_b state, which is not affected by ^{1}ET–^{1}LE mixing and undergoes electron-transfer reaction analogous to Figure 3a. On the other hand, ^{1}ET–^1L_a mixing is strong and ^{1}ET character of DMABN is advantageous on the ^{1}CT surface because the benzene radical anion derived from ^{1}ET–^1L_a mixing is further stabilized by Jahn-Teller distortion[31] to afford quinoid structure (Q).[32] Consequently ^1L_a – like and coplanar ICT state is smoothly shifted to stable TICT state with quinoid structure and exhibit so-called CT emission. It is still debatable whether or not excited DMABN initially populate TICT(Q) state via S_2/S_1 conical intersection and then undergo thermal equilibration with ^1L_b state.[30] Similarly, also D-π-A system based on binaphthyl has been reported to exhibit dual fluorescence comprised by $^1S_0$–^1L_b band and $^1S_0$–^{1}CT band.[33]

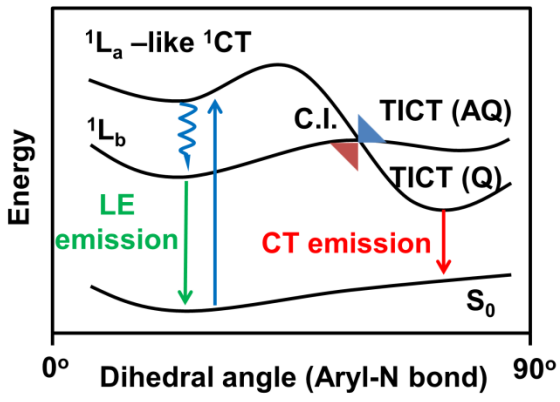

Figure 5. Schematic energy diagram of DMABN.[18] Straight lines represent radiative transitions and the wavy line indicates a non-radiative process. C.I. is conical intersection, Q and AQ mean quinoid and anti-quinoid structure of benzene anion radicals, respectively.

It is also noteworthy that TICT formations do not always impose weak fluorescence. As elucidated in the review by Grabowski, Rotkiewicz and Rettig,[30] if the structural relaxation of excited states involves more than one bond simultaneously, consequent TICT states have a chance to acquire sizable fluorescence quantum yields.[34] Recently, Yamaguchi and co-workers found a striking example of the hypothesis on *N*-borylated 2,5-diarylpyrroles (**1**).[35]

[a] Orbitals of *N*,*N*-dimethylamino and formyl group in Figure 4a can be replaced with HOMO of *N*,*N*-dimethylaniline and LUMO of benzaldehyde.

[b] Be advised that mesomeric interaction is a kind of electronic-state mixing and therefore all π-orbitals of the π-subsystems are subject to interactions. On the other hand, frontier-orbital interactions involve only HOMO and LUMO and their neighbouring orbitals. As a consequence, mesomeric interaction usually enhances a HOMO level of a π-system while frontier-orbital interactions usually result in lower HOMO level.

2. Material science based on the concept of TICT

Due to the ubiquitous nature of TICT phenomena, its concept has been applied to the development of various functional materials. Bulk of these researches employed TICT states just as "off states" of fluorescence probes. In contrast, several important researches in non-linear optics (NLO) and organic light-emitting diodes (OLEDs) addressed the essential aspect of TICT; they fully exploited the relationship between molecular geometries and ^{1}ET–^{1}LE mixing for their molecular designs.

2-1. Fluorescence probes for environmental polarity

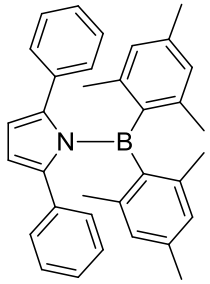

1

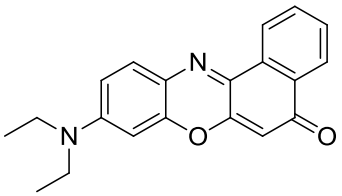

2

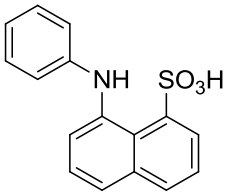

3

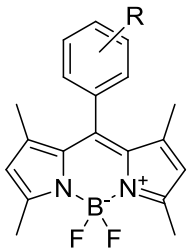

4

Because stronger ^{1}ET character translates into a more pronounced charge separation, TICT state are distinctly induced in polar environments and by substitution of strong donors and acceptors. Therefore, fluorescent molecules based on strong D-π-A systems are usually fluorescent in non-polar environments and experience fluorescence quenching in polar environments.[30] Nile red (**2**)[36] and 8-anilino-1-naphthalenesulfonic acid (ANS, **3**)[37] are famous polarity probes that are subject to polarity-caused quenching. However, it was also postulated that polarity-caused quenching of ANS (**3**) is ascribed to its photoionization.[38] Nile red (**2**) has been also a subject of fierce controversy about whether S_1 minimum is assigned to coplanar ICT or TICT.[39] In any case, their polarity-caused quenching, which is commonly observed for TICT-active molecules,[30] has been demonstrated to be useful for analyses of biological systems.[40-41] Nagano and co-workers developed the striking library of boron-dipyrromethene (BODIPY)-based environmental polarity sensors **4** whose donors, when the polarity of an environment surpassed a particular ON/OFF threshold, quenched the ^{1}LE fluorescence of BODIPY via electron-transfer reactions.[42] Since the transition dipole moment of ^{1}LE state of BODIPY and polarization of ^{1}ET state of **4** were perpendicular to each other, ^{1}ET–^{1}LE

mixing did not affect ^{1}LE fluorescence of BODIPY (Figure 3a) until just before the ON/OFF threshold.

2-2. Fluorescence probes for environmental viscosity

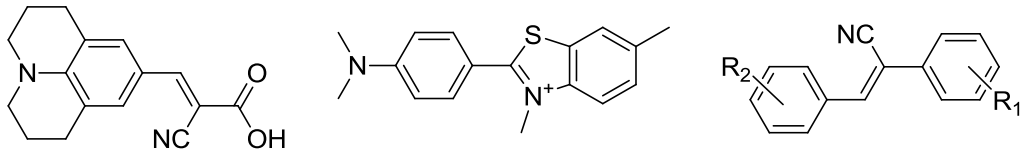

5 **6** **7**

Depending on the proportion of ^{1}ET and ^{1}LE character, directly connected D-π-A systems drastically change their fluorescence emission wavelengths, quantum yields, lifetimes, and spectral shapes. These dynamic characteristics are highly useful for fluorescence imaging of microviscosity, especially in biological systems. The particular class of fluorophores called "molecular rotors" can enhance their fluorescence intensity in sterically restricted environments such as viscous media.[43] Viscous environments make TICT-active fluorophores unable to overcome potential barriers against LE-TICT interconversions or in some cases, viscosity hampers internal conversion from TICT state. Representative molecular rotors are 9-(2-carboxy-2-cyanovinyl)julolidine (**5**) and its analogues,[44,45] whose versatilities have been demonstrated not only in molecular biology, such as in peptide-protein interaction studies,[46] and amyloid deposit research,[47] but also in polymer science,[48] contact mechanics,[49] and fluid dynamics.[50] Thioflavin-T **6** is a well-known TICT-based molecular rotor used *in vitro* cell biological and biomedical assays, especially in drug discovery assays and mechanistical studies with respect to amyloid-related neurodegenerative diseases.[51] α-Cyanostilbene derivatives **7** was recently emerged as a molecular rotor related to TICT phenomena.[52]

2-3. Fluorescence probes for specific chemical species

The presence of specific chemical species could also be visualised with TICT-active fluorophores such as RhoNox-1 **8**.[53] RhoNox-1 was the *N*-oxide derivative of Rhodamine B (Figure 6a) and normally exhibited weak fluorescence due to TICT formation, as depicted in the micrograph of Figure 6b. However, in the presence of Fe^{2+} ions, this *N*-oxide moiety in RhoNox-1 was selectively reduced to yield highly fluorescent Rhodamine B (Figure 6c).

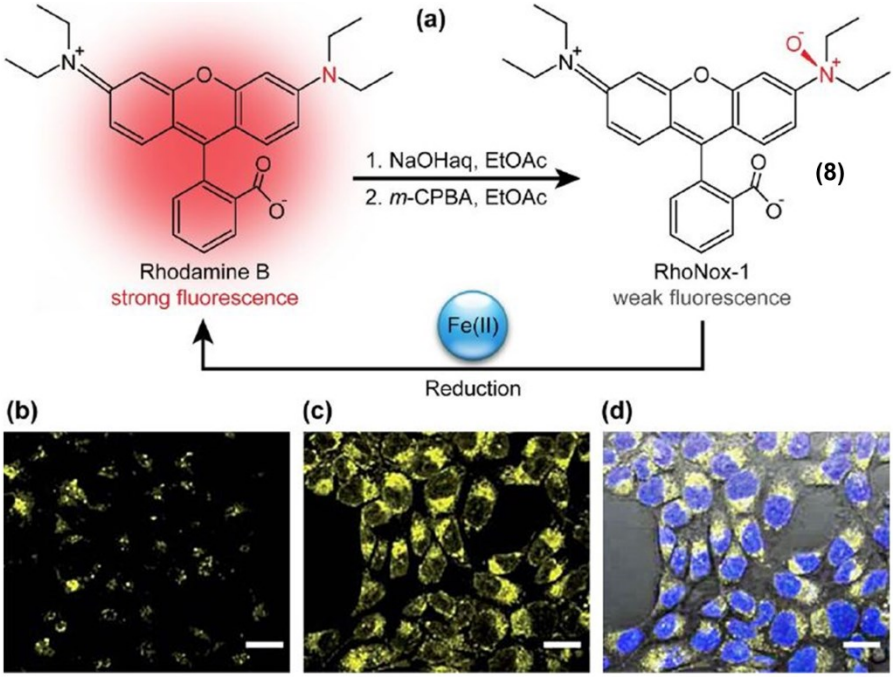

Figure 6. (a) Structure of RhoNox-1 **8** and the mechanism of iron(II)-ion detection; confocal fluorescence microscopy images of 5 μM RhoNox-1 (1 h, 37ºC) in HepG2 cells (b) under Control, and (c) after preincubation with 100 μM Fe(II) for 30 min; (d) bright field image merged with (c) and nuclear staining (Hoechst 3334) fluorescence micrographs. Bar: 20 μm.[53]

In another approach, Xie and co-workers developed "turn-on" CN^- probes (**9a–c**; Figure 7a) by introducing dicyanovinyl units at sterically demanding positions of large π frameworks, thereby forcing the moieties to twist out of the anthryl plane.[54] On such a highly *pretwisted* D-π-A system, the ^{1}ET character became dominant and the system's fluorescence was severely quenched through TICT formation. Nucleophilic addition of CN^- to dicyanovinyl groups disabled their electron-accepting abilities, and fluorescence was thus drastically enhanced (Figure 7b). These "turn-on" type fluorescent probes controlled the strengths of either donors or acceptors employing chemical reactions with analytes. Similar strategies have also been adopted in the development of hydrazine probes.[55-56]

Nakamura and co-workers adopted a significantly different approach to detect specific chemical species. They discovered that anthracene anilide derivatives underwent fluorescence quenching via TICT formation, which could partially be

suppressed in the presence of alkaline-earth-metal ions.[57] To amplify the sensitivity of anthracene anilides, two anthracene anilides were connected with a linear polyether (**10**; Figure 7c) in order to fixate its conformation and suppress torsional motion around the Ph-NH-CO- bond axis upon complexation with metal ions. As a consequence, **10** exhibited a 50–70-fold increase in its fluorescence intensity by the addition of Ca^{2+}, Sr^{2+} or Ba^{2+} ions.[58] This strategy, wherein complexation prevents TICT formation by imposing steric restriction, was also effective for the detection of neutral molecules such as surfactants.[59]

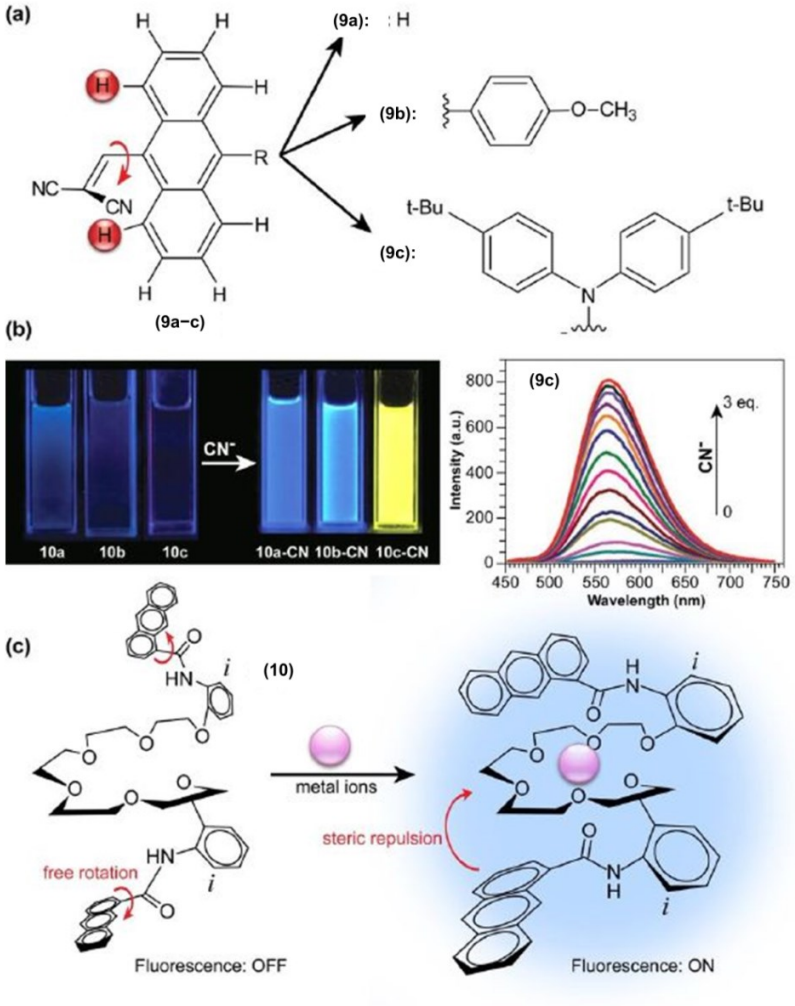

Figure 7. (a) Chemical structures of "turn-on" CN^- probes **9a-c**; (b) (left) digital photographs of 40 μM solution of **9a–c** under UV excitation in the absence and presence of CN^- (3 equiv.), (right) fluorescence changes upon addition of CN^- to **9c** (20 μM, λ_{ex} = 396 nm) in CH_2Cl_2;[54] (c) Proposed structural change of **10** in response to metal ions in the ground state.[58]

2-4. Aggregation-induced emission luminogens

Aggregation-induced emission luminogens (AIEgens) are a class of fluorophores that display subtle fluorescence in solution state, but are highly fluorescent in the aggregation state. Since AIEgens were expected to be promising materials for optoelectronic and bioimaging applications, there has been a vast amount of relevant research, as compiled and comprehensively discussed in recent reviews.[60-61] Typically, AIE phenomena are caused by restriction of intramolecular motions (RIM) accompanied by aggregation. Intramolecular motions are decisive also in the photophysics of TICT-active fluorophores; the proportion of ^{1}LE and ^{1}ET character at S_1 (global or local) minima, potential barriers against LE-TICT interconversions, and non-radiative transition rates of TICT states are all governed by steric environments around fluorophores.[30] Consequently, TICT-active fluorophores could be promising candidates for unique AIEgens with exceptional properties.

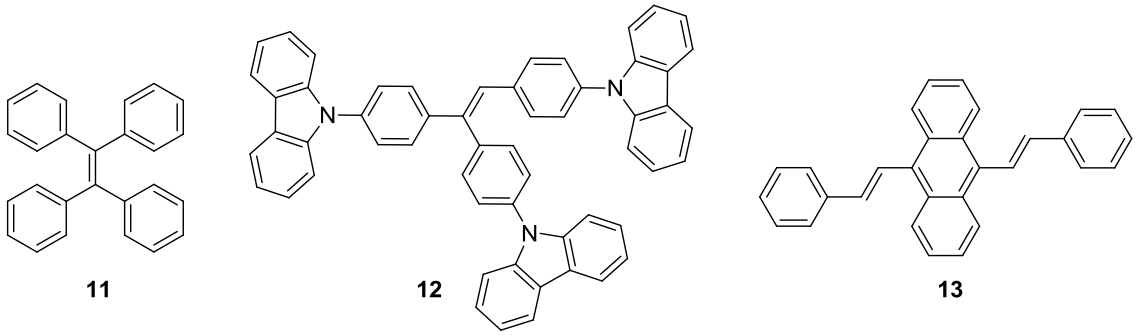

11 **12** **13**

In fact, tetraphenylethene (TPE; **11)**), one of the most famous AIEgen,[62] is known to undergo TICT formation in its excited state.[30,63-64] Stilbene analogues, such as TPE, often possess strong ^{1}ET character[30] and consequent TICT formations and fast non-radiative transitions can be inhibited by restriction of intramolecular rotation (RIR) of aggregation states. So far, many AIEgens have been designed based on stilbene structures, as exemplified by α-cyanostilbene derivatives **7**,[52] triphenylethene carbazole derivatives **12**,[65] and distyrylanthracene derivatives **13**.[66]

D-π-A systems based on BODIPY **4** were non-fluorescent in polar environments due to TICT formation, but recovered their fluorescence intensity upon aggregation.[67] Such a combination of polarity-caused quenching and AIE was also discovered in barbituric acid-functionalised tetraphenylethene derivatives (**14**; TPE-HPh-Bar; Figure 8), and revealed to be useful as optical waveguides.[68]

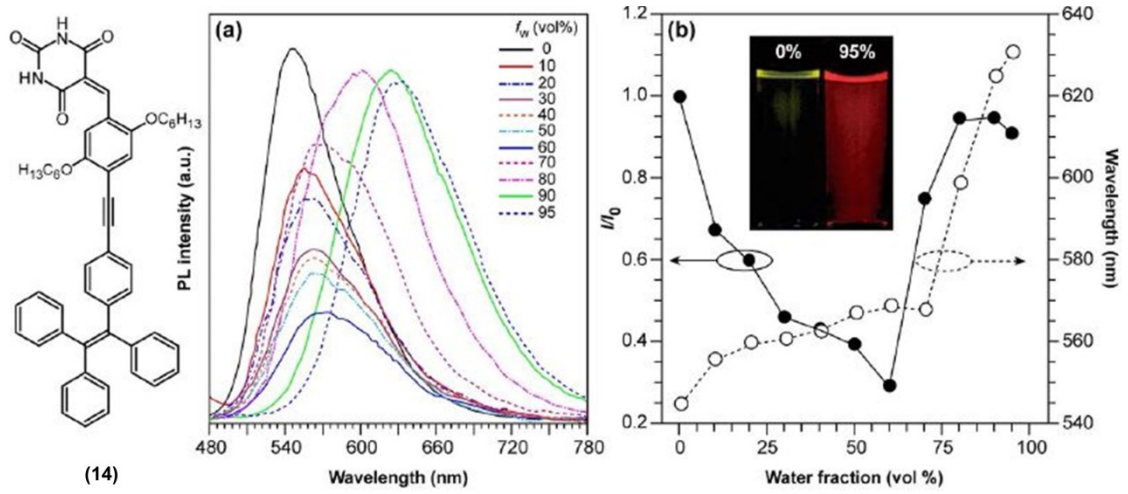

Figure 8. (a) Emission spectra of TPE-HPh-Bar **14** (λ_{ex} = 447 nm) in THF/water mixtures with different water fractions (f_w); (b) Plots of relative PL intensities (I/I_0) and emission maxima versus the composition of the THF/water mixture. I_0 = emission intensity in pure THF solution. Inset: Fluorescence emission of TPE-HPh-Bar in THF/water mixtures (0% and 95%) under UV excitation.[68]

2-5. Organic light emitting diodes

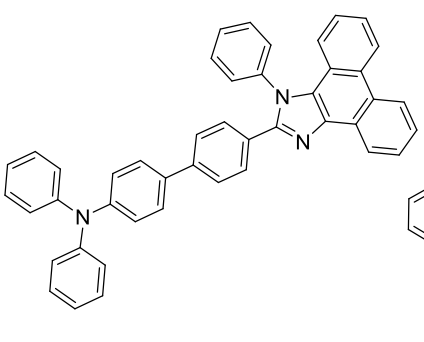

15

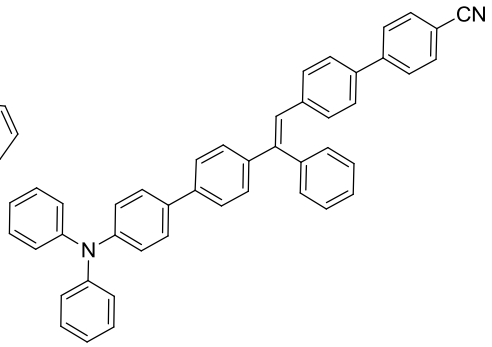

16

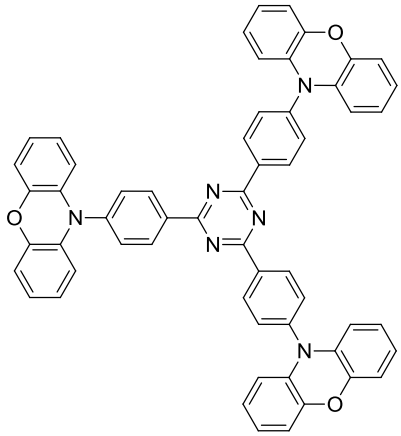

17

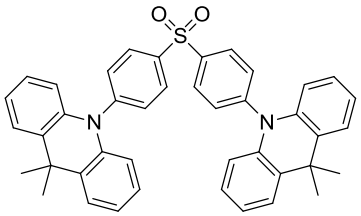

18

The competition between ^{1}LE character and ^{1}ET character plays an instrumental role in tuning the electronic structure of dopants. In organic light-emitting diodes (OLEDs), the recombination of injected holes and electrons produces a so-called charge-transfer (CT) exciton, which decays to generate one photon directly, or relaxes to a low-lying, and highly emissive locally excited (LE) exciton. To fully utilise both LE and CT excitons, Ma and co-workers designed the moderately twisted D-A system TPA-PPI **15**. Moderate torsion on TPA-PPI **15** optimized the proportion of ^{1}ET and ^{1}LE character at ^{1}CT minimum and consequently enabled ^{1}CT state not only to accept CT excitons but also to possess the large oscillator strength of LE excitons.[69] The strongly mixed state, where the energy levels of ^{1}LE and ^{1}ET states were closely arranged, had been called "hybridised local and charge transfer" (HLCT) state, which was regarded as an important strategy to enhance the electroluminescence efficiencies of OLEDs (Figure 9a).[70] On the course of HLCT study, it was also reported that the π-system where ^{1}ET−^{1}LE mixing was symmetry-forbidden exhibited lower photoluminescence quantum

yield but higher exciton utilization efficiency than its regioisomer where ^{1}ET–^{1}LE mixing was symmetry-allowed.[29]

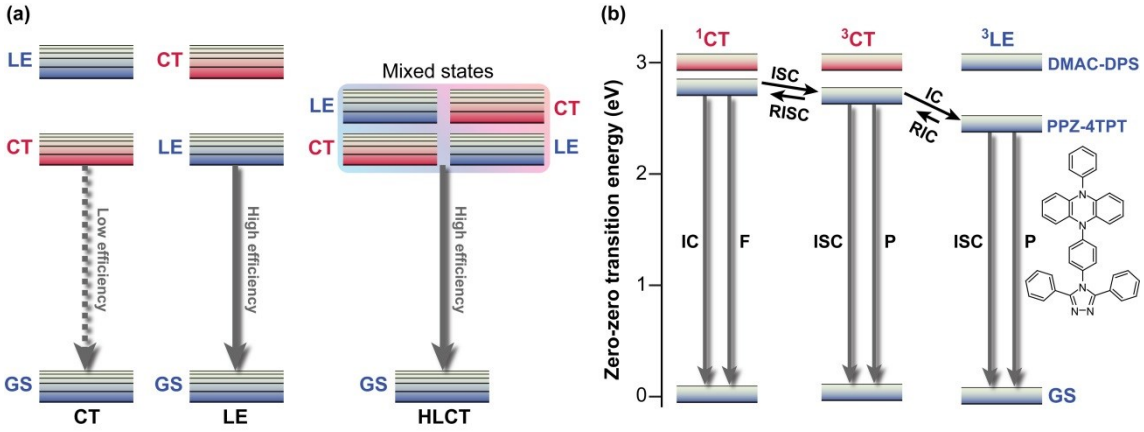

Figure 9. (a) Conceptual illustration of the three possible local excited (LE) and charge transfer (CT) state energy levels in donor-acceptor (D–A) molecules, *i.e.*, emission from CT, LE, and HLCT (hybridized local and charge transfer) states;[70] (b) Energy levels of PPZ–4TPT (4-[4-(5-phenyl-5,10-dihydrophenazine)phenyl]-3,5-diphenyl-1,2,4-triazole) and DMAC–DPS (bis[4-(9,9-dimethyl-9,10-dihydroacridine)phenyl]sulfone) calculated for toluene solution. F, fluorescence; P, phosphorescence; GS, ground state; IC, internal conversion; RIC, reverse internal conversion; ISC, intersystem crossing; RISC, reverse intersystem crossing.[74]

Electrons and holes possess degrees of freedom not only in orbitals, but also in their spin. Thus, to maximize the quantum efficiency of OLEDs, 25% of singlet excitons and 75% of triplet excitons, generated by arbitrary recombination of carriers, must be utilised as either fluorescence or phosphorescence. Thermally activated delayed fluorescence (TADF) paved the way for solving the problem;[71] highly *pretwisted* D-A systems minimized ^{1}CT-^{3}CT energy gaps due to the absence of electron-exchange interactions and initially populated ^{3}CT excitons were thus rapidly converted to their singlet counterparts. Therefore, TADF is compatible with TICT-active fluorophores. For example, *p*-TPA-3TPE-*p*-PhCN **16**, which achieved high external quantum efficiency over its theoretical value employing the TADF strategy, exhibited weak fluorescence in solution due to TICT formation and was highly emissive in the solid state.[72] Utilizing long-wavelength fluorescence of TICT states, colour tuning of TADF emitters were demonstrated on phenoxazine-substituted triphenyl-1,3,5-triazines (**17**).[73]

Recently, Adachi *et al*. achieved fast and efficient blue TADF based on engineering of ^{1}LE and ^{1}CT states.[74] Since ^{1}CT and ^{3}CT corresponding to blue emissions lie at relatively high energy levels, the lowest triplet state (T_1) tends to become a ^{3}LE state and hamper reverse intersystem crossing from ^{3}CT. To solve the problem of blue TADF, they arranged *pretwisted* D-A junctions at appropriate position (DMAC-DPS **18**) so as to destabilize the ^{3}LE state (Figure 9b). Taking Figure 4a for example, there are many D-A junction (*e.g.* N-aryl, aryl-aryl, and aryl-C (formyl) bonds) but only the torsion at the aryl-aryl effectively destabilizes ^{1}LE and ^{3}LE states. Thus ^{3}LE state of DMAC-DPS **18** was proximal to ^{3}CT and ^{1}CT states and underwent fast TADF. As a result, the device with **18** offered external quantum efficiency of up to 19.5%.

2-6. Nonlinear optics

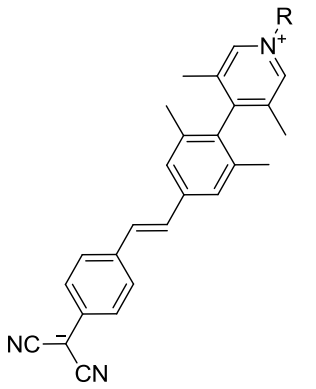

19

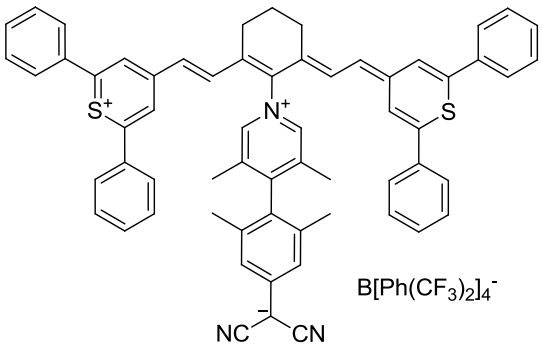

20

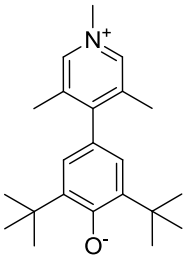

21

Recently, progress in nonlinear optics (NLO) revitalised TICT research. It may sound strange that TICT states, which are formed in excited-state adiabatic reactions, affect NLO properties of ground-state geometries. However, on highly *pretwisted* D-π-A systems, ^{1}ET-like states (*i.e.* TICT states) unquestionably exist with near-zero oscillator strengths and consequently affect NLO properties. In 1998, Ratner and co-workers theoretically predicted that highly twisted, but non-perpendicular, D-π-A systems would exhibit extraordinarily large second-order hyperpolarisabilities due to their minimal ^{1}LE characters in S_1 and large changes in dipole moments induced by photoexcitations.[75] This theoretical research had a significant impact on design strategies for NLO materials, because at that time conventional dogma dictated that planar, rigid, and large π-systems were desirable. These nearly perpendicular D-A systems, especially with zwitterionic structures, were named TICTOID chromophores.

In 2005, Marks *et al*. first reported the synthesis of a TICTOID-type dye, *i.e.*, "twisted π-electron system molecular chromophore" TMC-2 **19**.[76] TMC-2 displayed exceptional second-order hyperpolarisability β and electrooptical (EO) response, far surpassing those of existing dyes ($\mu\beta$ = –488000 × 10–48 esu).[76-77] Furthermore, TMC-2 was also shown to possess large third-order hyperpolarisability γ only in real part, equivalent to the nonlinear refractive index.[78] The effectiveness of TICTOID dyes is further demonstrated in various molecules, such as cyanine-TICTOID dyads **20**[79] and push-pull biphenyls **21**.[80]

2-7. Solar energy conversion with twisted D-A systems

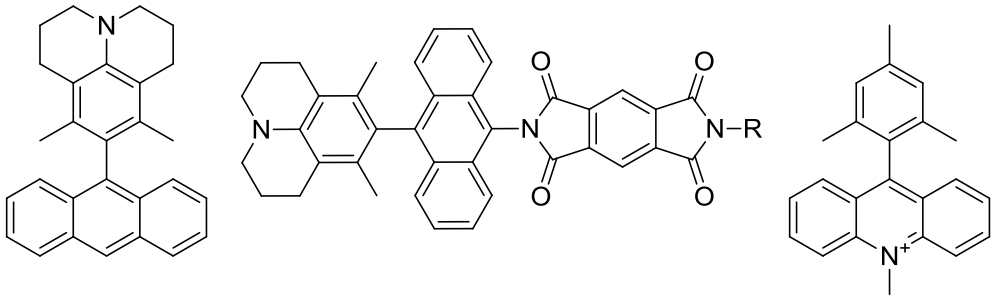

22 **23** **24**

To collect and store solar energy in a stable form, a pair of charges generated by photoexcitation must be collected at electrodes or stored through formation of chemical bonds. Not surprisingly, the long lifetime of photoexcited states enabled by charge separation or triplet state generation plays an instrumental role in solar energy conversions. Typically, charge separations have been studied in D-A systems in which the donor and acceptor were separated by an insulating bridge or spacer.

Parallel with research and developments in the TICT field, charge separation and transport dynamics were increasingly being studied also in directly bonded D-π-A systems. Wasielewski and collaborators examined charge separation dynamics in several twisted D-π-A systems (*e.g.* **22** and **23**) in which the donor and acceptor were directly bonded or connected by conjugating bridges.[81-82] As a result, they discovered spin-orbit, charge-transfer intersystem crossing (SOCT-ISC), where an electron experienced large fluctuation of its orbital angular momentum during a charge recombination, leading strong **^{1}CT-^{3}LE mixing** and **population of the ^{3}LE state**.

Fukuzumi and co-workers realized a long-lived charge-separation (CS) state with a singly bonded D-A pair, *i.e.*, 9-mesityl-10-methylacridinium (Acr^+–Mes; **24**). Acr^+–Mes kept its perpendicular conformation in the excited state[83] in spite of its weak donor, *i.e.* mesityl group. It may be attributed to severe *pretwisting* at the D-A junction, which makes ^{1}ET state advantageous. Furthermore, Acr^+–Mes was shown to be active in several photocatalytic reactions.[84]

3. Philosophy of this thesis

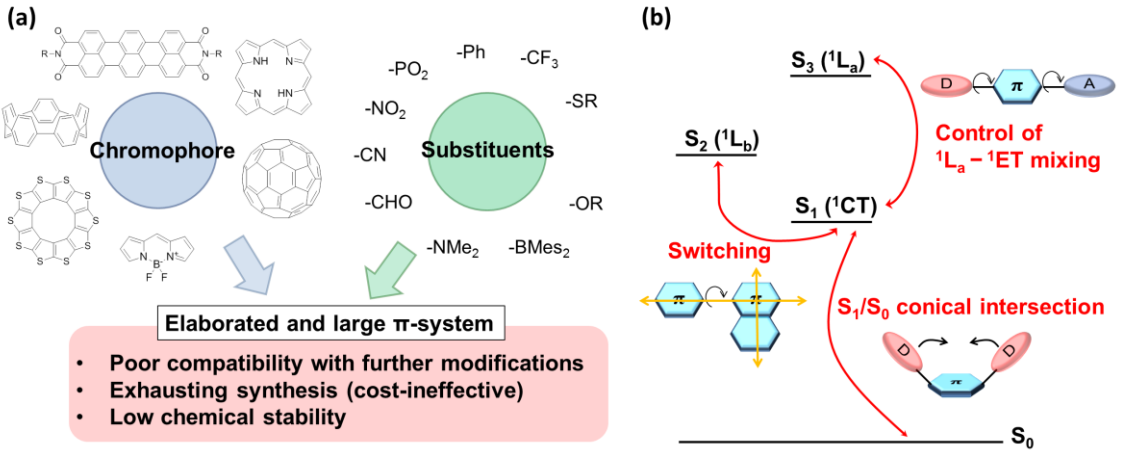

Figure 10. (a) Combinations of chromophores and substituents as an approach to attain desirable properties; (b) an electronic structure of typical D-π-A and D-π system. Interactions between each electronic state can be controlled by molecular geometries, which should bring about new functionality in conventional molecules.

As mentioned in the previous sections, **similar π-conjugated molecules** (*e.g.* identical chromophores or identical substituents) with different molecular geometries should exhibit **totally different** photophysical and photochemical properties. Nevertheless, most of conventional design strategies have primarily focused on combinations of chromophore and substituents (Figure 10a) and underestimated the effect of molecular geometry (especially of their conformations).[1-6] Taking environment-sensitive fluorophores for example,[2] while substituent effects such as strength of donors and acceptors or employments of unprecedented chromophores were widely examined, researches which explored desirable fluorescence properties by means of molecular geometries were quite limited. Also in other fields, design strategies often instructed us to adopt particular chemical species as exemplified in aryl-aryl bonds and stilbene-based structures for AIEgens,[60-61] *o*-nitrobenzyl, and several carbonyl compounds for photo-cleavable crosslinkers,[85] functionalized acenes[6] and heteroacenes[7b] for extension of π-conjugations. In this approach, the state-of-art dyes with superior photophysical and photochemical properties tend to have large and elaborated structures, of which syntheses are usually exhausting. Additionally, as π-conjugated molecules become larger and structurally more complicated, further

functionalizations (*e.g.* bioconjugation, improving processability for device fabrications) get more difficult. Therefore any alternative approach, to realize superior functionalities based on conventional chromophores (*e.g.* benzene, naphthalene, anthracene, biphenyl ⋯) with only a few and simple substituents, is desired.

This thesis, in contrast to the conventional approach, adopted **a molecular geometry** as a primary player on the design of π-conjugated molecules rather than chromophore and substituents. Chromophores appeared in this thesis were quite conventional, *i.e.* naphthalene, anthracene, pyrene and binaphthyl. This thesis elucidated what molecular geometries should induce or modulate superior photophysical and photochemical functions. Comparing with the terminologies such as "functional chromophore" and "functional group", such a particular geometries (or conformations) could be referred to as "**functional geometry**". To create functional geometries, this thesis utilized interaction, coupling, and mixing between various excited states of D-π-A and D-π systems (Figure 10b). As described in section 1-3, 1-4, ^{1}ET–^{1}LE mixing could be modulated by torsion not only at D-A junctions, but also at adjacent bonds to afford desirable ^{1}CT state. In addition, another ^{1}LE state whose ^{1}ET–^{1}LE mixing was symmetry forbidden might exhibit switching behaviour between ^{1}CT state. Also this thesis challenged engineering of S_1/S_0 conical intersections (CI) where S_1 states were proximate to S_0 state. As a result, it was revealed that strongly twisted donors at adequate positions of polycyclic aromatic hydrocarbons (PAHs) stabilize their S_1/S_0 CI, affording drastic AIE and viscosity-sensitive fluorescence.

4. Abstracts for this thesis

Chapter 2. Fluorescence Solvatochromism and Dual-mode Fluorescence Controlled by Torsional Restrictions at Donor-acceptor Junctions.

In this chapter, the relationship between torsion at a D-A junction and ^{1}ET–^{1}LE mixing, which was illustrated in Figure 4, are employed for the design of fluorescent dyes. In the chapter 2-1, push-pull biphenyl analogs (4-(*N*,*N*-dimethylamino)-4'-formyl biphenyl) with a modulated dihedral angle of the aryl-aryl bond, using a bridged structure or methyl groups, were synthesized. Photophysical measurements of these synthesized compounds revealed the effect of the torsion between *N*,*N*-dimethylaniline (donor) and benzaldehyde moieties (acceptor) on their solvatochromic properties. Obtained data showed that the sensitivity of the fluorescence maxima to solvent polarity (fluorescence solvatochromism) gradually increased as the biphenyl chromophore was restricted to a twisted conformation. In polar environments highly twisted biphenyls exhibited slow components on fluorescence lifetime, which indicated the existence of highly polarized ^{1}CT state with dominant ^{1}ET character. On the other hand, less twisted push-pull biphenyls that were unlikely to populate TICT state also displayed stepwise enhancement of excited-state polarizations and fluorescence lifetimes as the torsion at the aryl-aryl bond slightly increased. Thus the study successfully developed two disparate solvatochromic probes just by imposing steric restrictions; one was brightly fluorescent and suitable for biosensing and living cell imaging, and another featured fluorescent at particular polarity region and unprecedentedly large solvatochromism, which was suitable for imaging of microenvironments (*e.g.* lipid rafts).

In chapter 2-2, ^1L_b state was involved as another actor on the twisted D-π-A system. ^1L_b state of naphthalene could not be mixed efficiently with ^{1}CT state created by ^{1}ET–^1L_a mixing and additionally, the energy level of ^1L_b state still remained to be comparable to ^{1}CT state unless strong donor or strong acceptor was introduced on the naphthalene. Thus dual fluorescence from ^{1}CT and ^1L_b states was reported.[33] Utilizing the features, this study developed aggregation-induced emission active D-π-A binaphthyl with dual-mode fluorescence; this dye exhibited yellow aggregation-induced emission (AIE) with enhanced co-planarity but showed blue $S_0 \leftarrow {}^1L_b$ fluorescence in a glassy solvent (77 K, toluene) with twisted conformation. AIE was not observed

without donor-acceptor functionalization of binaphthyl and strongly polarized ^{1}CT state was confirmed to activate AIE. The dual modes of photophysical function, *i.e.* AIE of ^{1}CT state and fluorescence thermochromism by ^{1}CT−^1L_b interconversion, was unprecedented on such a simple molecule as the D-π-A binaphthyl.

Chapter 3. Directional Control of π-Conjugation Enabled by Distortion of the Donor Plane in Diarylaminoanthracenes

In this chapter, the framework of ^{1}ET−^{1}LE mixing was applied to extension of π-conjugation. In the conventional notion, the dogmatic strategy to maximize π-conjugation is to increase the co-planarity of the π-skeleton. However high co-planarity of a π-skeleton must compromise solubility problems on synthesis, purification and processing. Thus this chapter proposes the alternative strategy for π-extension; the distortion of a local π-plane in bichromophoric or higher-complexity systems should extend their π-conjugation rather than undermine it. The hypothesis should be possible from the theoretical aspect because distortion of a donor plane destabilizes electron-transfer (^{1}ET) state and prompt state mixing between ^{1}ET and locally excited (^{1}LE) state. As a model system, the author designed and synthesized a series of diarylaminoanthracenes in which the planarity of the diarylamine moiety is controlled by methylene- or ethylene- bridges. The X-ray crystallographic structures confirmed that the methylene- and ethylene bridges gradually decreased the disorder of the diarylamine planes. Photophysical measurements revealed that enhanced planarity of the diarylamine moiety optically forbade the charge-transfer transition between the diarylamine and anthracene moieties. Density functional theory calculations further illustrate that the frontier orbitals of diarylamine and anthracene interpenetrate as the donor plane is distorted. Additionally, natural bonding orbital analyses reveal that distortion of the donor plane changes the directionality of the π-conjugation of the nitrogen n-orbital from intrachromophoric to interchromophoric.

Chapter 4. Steric-environment Sensitivity of Fluorescence Activated by Twisted N,N-dialkylamino groups

Chapter 4 was the proposition of the novel design strategy to activate conventional aromatic hydrocarbons as aggregation-induced emission luminogens (AIEgens) and fluorescence molecular rotors. In chapter 4-1, a series of regioisomers of piperidylanthracenes (**PA**) and bis(piperidyl)anthracenes (**BPA**) were synthesized and their photophysical properties examined in solution, suspension, and the solid state. Aggregation-induced emission (AIE) was observed only for **1,4-BPA** and **9,10-BPA**, in which two piperidyl groups are substituted at the anthracene moiety in *para*-position with respect to each other. Compared to previously reported AIE luminogens, these easily obtainable *para*-substituted **BPA**s, exhibited several unique and beneficial features, such as simple structures, bright solid-state fluorescence (Φ_{fl} = 0.49 and 0.86 for **1,4-BPA** and **9,10-BPA**, respectively), tunable fluorescence emission, and large Stokes shifts. Results from diffuse-reflectance and fluorescence lifetime measurements demonstrated that **PAs** and **BPAs** intrinsically possess an efficient non-radiative transition pathway in the solid state, and that **1,4-BPA** and **9,10-BPA** may overcome this pathway. The X-ray crystallographic analysis of **1,4-BPA** revealed that undesirable interchromophoric interactions can be minimised. DFT and TD-DFT calculations suggested that severe coulomb repulsion between lone pairs of confronting piperidyl groups, which was absent presumably due to electronic correlations, enhanced the stokes shift of **1,4-BPA**. The Aryl-N rotation accompanied by the large stokes shift of **1,4-BPA** was sufficiently small to complete its relaxation even in solid states, which should result in the absence of self-absorption.

Chapter 4-2 proceeded into more essential question; how *N*,*N*-dialkylamino group made anthracene ring non-fluorescent in common organic solvents and highly fluorescent in solid states, only when they are introduced at 1,4- and 9,10-positions. The joint project with theoretical chemists revealed that the introduction of highly twisted *N*,*N*-dialkylamines into an anthracene ring results in two ^{1}CT minima with different symmetry and Aryl-N planarity, which in turn lead to prominent Stokes shifts and efficient solid-state fluorescence. Furthermore, *para*-substitution of donors on an aromatic hydrocarbon proved to be an effective strategy for designing steric-environment sensitive fluorophores. Donor moieties that face each other stabilize

the S_1/S_0 minimum energy conical intersection (MECI) of anthracene and other typical aromatic hydrocarbons, and thus internal conversion become fast in solution state but was suppressed in solid state or viscous media. These design strategy, *i.e.* highly twisted *N*,*N*-dialkylamines in *para*-orientation was successfully applied for activation of a naphthalene ring to achieve aggregation-induced emission and viscosity-sensitive fluorescence. This study also scrutinized the effects of the alkyl-chain flexibilities of 9,10-bis(*N*,*N*-dialkylamino)anthracenes (**BDAA**) on the absorption of these compounds. Contrary to popular notions, large and flexible alkyl chains, such as isobutyl groups, allow for planarity around the C-N bond of **BDAA** rather than small and stiff alkyl groups such as methyl groups.

Chapter 4-3 applied the design strategy for simple AIEgens to pyrene chromophore; strongly twisted *N*,*N*-dialkylamines should stabilize S_1/S_0 MECI of pyrene, yielding faint fluorescence in solution states but strong fluorescence in solid states. In Chapter 4-1 and Chapter 4-2, strongly twisted *N*,*N*-dialkylamine was found to best activate AIE when they are introduced at 1,4-position of naphthalene and 9,10-position of anthracene. However these positions of naphthalene and anthracene not only stabilize their S_1/S_0 MECI but also induce strong interaction between donor moieties and aromatic hydrocarbons even at S_1 and S_0 minima due to the largest AO coefficient. In contrast, Maeda *et al*. reported that deformation at 2- and 4-position of pyrene stabilize its S_1/S_0 CI more than deformation at 1-position,[86] which possesses the largest AO coefficient. Thus it is expected that strongly twisted *N*,*N*-dialkylamines at 4-position of pyrene exclusively activate AIE while those at 1-positions does not. In this chapter, 1-(*N*,*N*-dimethylamino)pyrene (**1-Py**), 1,6-bis(*N*,*N*-dimethylamino)pyrene (**1,6-Py**), 4-(*N*,*N*-dimethylamino)pyrene (**4-Py**), 1-(*N*,*N*-dimethylamino)pyrene (**4,5-Py**). While **1-Py**, **1,6-Py** and **4-Py** were more or comparably fluorescent in solution state than in solid state, **4,5-Py** exhibited faint fluorescence in solution state ($\Phi_{fl} \approx 0.06$ in methanol) but strong fluorescence in solid state ($\Phi_{fl} \approx 0.49$). These result emphasizes the importance of stabilization of S_1/S_0 MECI rather than electronic interaction between *N*,*N*-dimethylamine and pyrene chromophore.

Chapter 5. Terminal Functionalization of bis(N,N-dialkylamino)arenes and its Application for Fluorescence Thermometer

In Chapter 4, superiorities of 9,10-bis(*N*,*N*-dialkylamino)anthracene (**BDAA**) and 1,4-bis(*N*,*N*-dialkylamino)-2,3-dimethylnaphthalene (**DMe-BDAN**) as AIEgens were demonstrated. As I noted in the philosophy section, excellent functional fluorophores must be functionalized in facile way. However, introduction of *N*,*N*-dialkylamine at sterically congested position of aromatic hydrocarbons have been explored much less than unhindered aromatic hydrocarbons. Therefore this chapter developed syntheses of **BDAA** and **DMe-BDAN** with hydroxy groups at their terminal positions. As a result, 9,10-bis(*N*-(3'-(*N*''-(3''-hydroxyprop-1''-yl)-*N*''-methylamino))prop-1'-yl)-*N*-methyla mino)anthracene (**BDAA-OH**) was successfully synthesized by the three-step reaction (Yield 53%) from 9,10-dibromoanthracene, while 1,4-bis(*N*-(hydroxypent-5-yl) -*N*-methylamino)-2,3-dimethylnaphthalene (**DMe-BDAN-OH**) was prepared by the four-step reaction (Yield 65%) from 2,3-dimethylnaphthalene. To examine the potential as functional materials, **BDAA-OH** and **DMe-BDAN-OH** were further modified with methacrylate moieties to employ them as the monomers and the crosslinkers. The prepared monomers and crosslinkers were used for co-polymerization to yield Poly(*N*-isopropylacrylamide) and those gels. At 20 ^{o}C, PNIPAM based on **BDAA** exhibited faint fluorescence in THF (Φ_{fl} = 0.05) and water ($\Phi_{fl} \leq 0.11$), whreas those based on **DMe-BDAN** showed quite stronger fluorescence both in THF ($\Phi_{fl} \approx 0.32$) and in water ($\Phi_{fl} \approx 0.55$) than the corresponding monomer. Thus PNIPAM based on **BDAA** exhibited steep increase of fluorescence intensity and Φ_{fl} around 27 – 35 ^{o}C, while PNIPAM based on **DMe-BDAN** showed monotonic decrease of fluorescence intensity and Φ_{fl} as temperature rised. PNIPAM gels based on **BDAA** and **DMe-BDAN** did not indicate significant temperature dependence of fluorescence quentum yields. There results suggests that PNIPAM based on **BDAA** can be applied to fluorescence thermometer, whereas PNIPAM-induced fluorescence enhancement of **DMe-BDAN** fluorophore is intriguing from the fundamental aspect.

Chapter 6. A Structurally Simple Bis(piperidyl)naphthalene Cross-linker Exhibiting Fluorescence Quenching and Photodegradation in Trichloromethyl–Containing Chloroalkanes

Chapter 4-1 revealed that moderately twisted *N*,*N*-dialkylamino groups in *para*-relationship greatly elevate HOMO levels of aromatic hydrocarbons during excited-state relaxation processes. This phenomenon implies that *para*-disubstituted bis(*N*,*N*-dialkylamino)arene may be subject to rapid oxidation only after photoexcitation. Therefore, in this chapter, 1,4-bis(piperidyl)naphthalene (**1,4-BPN**) was employed as a cross-linker for poly(*n*-butyl methacrylate) gels to generate soft materials that undergo fluorescence quenching and photodegradation selectively in 1,1,1-trichloromethyl-containing chloroalkanes. In chloroform and 1,1,1-trichloroethane, **1,4-BPN** underwent efficient fluorescence quenching *via* exciplex formation, resulting in rapid photodegradation. Similarly, poly(*n*-butyl methacrylate) gels crosslinked with **1,4-BPN** were highly fluorescent and stable in various organic solvents and chloroalkanes, but exhibited less intense fluorescence and rapid photodegradation in 1,1,1-trichloromethyl-containing chloroalkanes. The thus obtained gels exhibited a steep drop in the storage modulus during first 10 seconds of photoirradiation (λ = 365 nm) upon swelling in 1,1,1-trichloroethane. Further photoirradiation for 10-30 minutes led to the decomposition of the gel. Thus, I propose that this **1,4-BPN**-based cross-linker could be used for the facile preparation of diverse polymeric materials with synergistic fluorescence, detection, and photodecomposition properties towards unreactive and neutral analytes.

5. References

1. Anthony, J. E. *Chem. Rev.* **2006**, *106*, 5028–5048.
2. Yang, Z.; Cao, J.; He, Y.; Yang, J. H.; Kim, T.; Peng, X.; Kim, J. S. *Chem. Soc. Rev.* **2014**, 43, 4563-4601.
3. He, G. S.; Tan, L. S.; Zheng, Q.; Prasad, P. N. *Chem. Rev.* **2008**, *108*, 1245–1330.
4. Li, X.; Gao, X.; Shi, W.; Ma, H. *Chem. Rev.* **2014**, *114*, 590-659.
5. Kawata, S.; Kawata, Y. *Chem Rev.* **2000**, *100*, 1777-1788.
6. Ravelli, D.; Fagnoni, M.; Albini, A. *Chem. Soc. Rev.* **2013**, *42*, 97-113.
7. (*a*) Shen, Y.; Chen, C.-F. *Chem. Rev.* **2012**, *112*, 1463-1535; (*b*) Fukazawa, A.; Yamaguchi, S. *Chem. Asian. J.* **2009**, *4*, 1386–1400; (*c*) Ito, S.; Hiroto, S.; Lee, Sangsu, Son, M.; Hisaki, I.; Yoshida, T.; Kim, D.; Kobayashi, N.; Shinokubo, H. *J. Am. Chem. Soc.* **2015**, *137*, 142-145.
8. Da Silva, E. C.; Gerratt, J.; Cooper, D. L.; Raimondi, M. *J. Chem. Phys.* **1994**, *101*, 3866-3887.
9. (*a*) Beck, S. M.; Powers, D. E.; Hopkins, J. B.; Smalley, R. E. *J. Chem. Phys.* **1980**, *73*, 2019-2028; (*b*) Robey, M. J.; Ross, I. G.; Southwood-Jones, R. V.; Strickler, S. J. *Chem. Phys.* **1977**, *23*, 207-216.
10. (*a*) Bayliss, N. S. *J. Chem. Phys.* **1948**, *16*, 287-292; (*b*) Kuhn, H. *J. Chem. Phys.* **1948**, *16*, 840-841.
11. (*a*) Simpson, W. T. *J. Chem. Phys.* 1949, 17, 1218-1221; (*b*) Baerends, E. J.; Ricciardi, G.; Rosa, A.; van Gisbergen, S. J. A. *Coord. Chem. Rev.* **2002**, *230*, 5-27.
12. Platt, J. R. *J. Chem. Phys.* **1949**, *17*, 484-495.
13. Steiner, R. P.; Michl, J. *J. Am. Chem. Soc.* **1978**, *100*, 6861-6867.
14. Hiraya, A.; Shobatake, K. *J. Chem. Phys.* **1991**, *94*, 7700-7706.
15. Schreiber, M.; Silva-Junior, M. R.; Sauer, S. P. A.; Thiel, W. *J. Chem. Phys.* 2008, 128, 134110.
16. Huebner, R. H.; Mielczarek, S. R.; Kuyatt, C. E. *Chem. Phys. Lett.* **1972**, *16*, 464-469.
17. Kimura, K.; Tsubomura, H.; Nagakura, S. *Bull. Chem. Soc. Jpn.* **1964**, *37*, 1336-1346.
18. Cogan, S.; Zilberg, S.; Haas, Y. *J. Am. Chem. Soc.* **2006**, *128*, 3335-3345.

19. Yamaguchi, H.; Ikeda, T.; Mametsuka, H. *Bull. Chem. Soc. Jpn.* **1946**, *49*, 1762-1765.

20. Rettig, W.; Wermuth, G. *J. Photochem.* **1985**, *28*, 351-366.

21. Marcus, R. A.; Sutin, N. *BioChim. Biophys. Acta - Bioenergetics* **1985**, *811*, 365-322.

22. (*a*) Marcus, R. A. *J. Phys. Chem.* **1989**, *93*, 3078-3086; (*b*) Marcus, R. A. *J. Chem. Phys.* **1965**, *43*, 1261.

23. Turro, N.; Ramamurthy, V.; Scaiano, J. C. *Modern Molecular Photochemistry of Organic Molecules*; University Science books: Sausalito, **2010**; pp 257-259.

24. Mulliken, R. S. *J. Am. Chem. Soc.* **1952**, *74*, 811-824.

25. Murrell, J. N. *J. Am. Chem. Soc.* **1959**, *81* 5037-5043.

26. Mulliken, R. S.; Person, W. B. *Molecular Complexes: A Lecture and Reprint Volume*; Wiley; New York, **1969**.

27. Mataga, N.; Murata, Y. *J. Am. Chem. Soc.* **1969**, *91*, 3144-3152.

28. Herbich, J.; Kapturkiewicz, A. *J. Am. Chem. Soc.* **1998**, *120*, 1014-1029.

29. Wang, Z.; Feng, Y.; Zhang, S.; Gao, Y.; Gao, Z.; Chen, Y.; Zhang, X.; Ping, L.; Yang, B.; Chen, P.; Ma, Y.; Liu, S. *Phys. Chem. Chem. Phys.* **2014**, *16*, 20772-20779.

30. Grabowski, Z. R.; Rotkiewicz, K.; Rettig, W. *Chem Rev*. **2003**, *103*, 3899-4032.

31. Jahn, H. A.; Teller, E. *Proc. Roy. Soc. (London)* **1937**, *A161*, 220-235.

32. Hinde, A. L.; Poppinger, D.; Radom, L. *J. Am. Chem. Soc.* **1978**, *100*, 4681-4685.

33. Lahmani, F.; Breheret, E.; Z.-Rentien, A.; Amatore, C.; Jutand, A. *J. Photochem. Photobiol. A: Chem.* **1993**, *70*, 39-49.

34. Lapoude, R.; Czeschka, K.; Majenz, W.; Rettig, W.; Gilabert, E.; Rulliere, C. *J. Phys. Chem.* **1992**, *96*, 9643-9650.

35. Taniguchi, T.; Wang, J.; Irie, S.; Yamaguchi, S. *Dalton Trans.* **2013**, *42*, 620-624.

36. Dutta, A. K.; Kamada, K.; Ohta, K. *J. Photochem. Photobiol. A: Chem.* **1996**, *93*, 57-64.

37. Kosower, E. M.; Dodiuk, H.; Kanety, H. *J. Am. Chem. Soc.* **1978**, *100*, 4179-4188.

38. Robinson, G. W.; Robbins, R. J.; Fleming, G. R.; Morris, J. M.; Knight, A. E. W.; Morrison, R. J. S. *J. Am. Chem. Soc.* **1978**, *100*, 7145-7150.

39. Guido, C. A.; Menucci, B.; Jacquemin, D.; Adamo, C. *Phys. Chem. Chem. Phys.* **2010**, *12*, 8016-8023.

40. Slavik, J. *BioChim. Biophys. Acta – Biomembranes* **1982**, *694*, 1-25.

41. Prifti, E.; Reymond, L.; Umebayashi, M.; Hovius, R.; Riezman, H.; Johnsson K. *ACS Chem. Biol.* **2014**, *9*, 606-612.

42. Sunahara, H.; Urano, Y.; Kojima, H.; Nagano, T. *J. Am. Chem. Soc.* **2007**, *129*, 5597-5604.

43. Haidekker, M. A.; Theodorakis, E. A. *Org. Biomol. Chem.* **2007**, *5*, 1669-1678.

44. Haidekker, M. A.; Theodorakis, E. A. *J. Biol. Eng.* **2010**, *4*, 11.

45. Sutharsan, J.; Dakanali, M.; Capule, C. C.; Haidekker, M. A.; Yang, J.; Theodorakis, E. A. *ChemMedChem*. **2010**, *5*, 56-60.

46. Goh, W. L.; Lee, M. Y.; Joseph, T. L.; Quah, S. T.; Brown, C. J.; Verma, C.; Brenner, S.; Ghadessy, F. J.; Teo, Y. N. *J. Am. Chem. Soc*. **2014**, *136*, 6159-6162.

47. Cao, K.; Farahi, M.; Dakanali, M.; Chang, W. M.; Sigurdson, C. J.; Theodorakis, E. A.; Yang, J. *J. Am. Chem. Soc*. **2012**, *134*, 17338-17341.

48. Priestley, R. D.; Ellison, C. J.; Broadbelt, L. J. Torkelson, J. M. *Science* **2005**, *309*, 456-459.

49. Suhina, T.; Weber, B.; Carpentier, C. E.; Lorincz, K.; Schall, P.; Bonn, D.; Brouwer, A. M. *Angew. Chem. Int. Ed.* **2015**, *54*, 3688-3691.

50. Mustafic, A.; Huang, H. M.; Theodorakis, E. A.; Haidekker, M. A. *J. Fluoresc*. **2010**, *20*, 1087-1098.

51. Amdursky, N.; Erez, Y.; Huppert, D. *Acc. Chem. Res.* **2012**, *45*, 1548-1557.

52. Zhu, L.; Zhao, Y. *J. Mater. Chem. C* **2013**, *1*, 1059-1065.

53. Hirayama, T.; Okuda, K.; Nagasawa, H. *Chem. Sci*. **2013**, *4*, 1250-1256.

54. Chen, B.; Ding, Y.; Li, X.; Zhu, W.; Hill, J. P.; Ariga, K.; Xie, W. *Chem. Commun.* **2013**, *49*, 10136-10138.

55. Zhou, D.; Wang, Y.; Jia, J.; Yu, W.; Qu, B.; Li, X.; Sun, X. *Chem. Commun.* **2015**, *51*, 10656-10659.

56. Chen, B.; Sun, X.; Li, X.; Agren. H.; Xie, Y. *Sensor Actuat. B-Chem.* **2014**, *199*, 93-100.

57. Morozumi, T.; Anada, T.; Nakamura, H. *J. Phys. Chem. B* **2001**, *105*, 2923-2931.

58. Kim, J.; Morozumi, T.; Hiraga, H.; Nakamura, H. *Anal. Sci.* **2009**, *25*, 1319-1325.

59. Oka, Y.; Nakamura, S.; Morozumi, T.; Nakamura, H. *Talanta* **2010**, *82*, 1622-1626.
60. Hong, Y.; Lam, J. W. Y.; Tang, B. Z. *Chem. Soc. Rev.* **2011**, *40*, 5361-5388.
61. Mei, J.; Hong, Y.; Lam, J. W. Y.; Qin, A.; Tang, Y.; Tang, B. Z. *Adv. Mater.* **2014**, *26*, 5429-5479.
62. Dong, Y.; Lam, J. W. Y.; Qin, A.; Sun, J.; Liu, J.; Li, Z.; Zhang, S.; Sun, J.; Kwok, H. S.; Tang, B. Z. *Appl. Phys. Lett.* **2007**, *91*, 011111.
63. Schilling, C. L.; Hilinski, E. F. *J. Am. Chem Soc.* **1988**, *110*, 2296-2298.
64. Tahara, T.; Hamaguchi, H. *Chem. Phys. Lett.* **1994**, *217*, 369-374.
65. Yang, Z.; Chi, Z.; Yu, T.; Zhang, X.; Chen, M.; Xu, B.; Liu, S.; Zhang, Y.; Xu, J. *J. Mater. Chem.* **2009**, *19*, 5541-5546.
66. He, J.; Xu, B.; Chen, F.; Xia, H.; Li, K.; Ye, L.; Tian, W. *J. Phys. Chem. C* **2009**, *113*, 9892-9899.
67. Hu, R.; Lager, E.; Aguilar, A. A.; Liu, J.; Lam, J. W. Y.; Sung, H. H. Y.; Williams, I. D.; Zhong, Y.; Wong, K. S.; P.-Cabrera, E.; Tang, B. Z. *J. Phys. Chem. C* **2009**, *113*, 15845-15853.
68. Wang, E.; Lam, J. W. Y.; Hu, R.; Zhang, C.; Zhao, Y. S.; Tang, B. Z. *J. Mater. Chem. C* **2014**, *2*, 1801-1807.
69. Li, W.; Liu, D.; Shen, F; Ma, D.; Wang, Z.; Feng, T.; Xu, Y.; Yang, B.; Ma, Y. *Adv. Funct. Mater.* **2012**, *22*, 2797-2803.
70. Li, W.; Pan, Y.; Yao, L.; Liu, H.; Zhang, S.; Wang, C.; Shen, F.; Lu, P.; Yang, B.; Ma, Y. *Adv. Opt. Mater.* **2014**, *2*, 892-901.
71. Uoyama, H.; Goushi, K.; Shizu, K.; Nomura. H.; Adachi, C. *Nature* **2012**, *492*, 234-238.
72. Li, J.; Jiang, Y.; Cheng, J.; Zhang, Y.; Su, H.; Lam, J. W. Y.; Sung, H. H. Y.; Wong, K. S.; Kwok, H. S.; Tang, B. Z. *Phys. Chem. Chem. Phys.* **2015**, *17*, 1134-1141.
73. Tanaka, H.; Shizu, K.; Nakanotani, H.; Adachi, C. *Chem. Mater.* **2013**, *25*, 3766-3771.
74. Zhang, Q.; Li, B.; Huang, S.; Nomura, H.; Tanaka, H.; Adachi, C. *Nat. Photonics* **2014**, *8*, 326-332.
75. Albert, I. D. L.; Marks, T. J.; Ratner, M. A. *J. Am. Chem. Soc.* **1998**, *120*, 11174-11181.

76. Kang, H.; Facchetti, A.; Zhu, P.; Jiang, H.; Yang, Y.; Cariati, E.; Righetto, S.; Ugo, R.; Zuccacia, C.; Macchioni, A.; Siern, C. L.; Liu, Z.; Ho, S.-T.; Marks, T. J. *Angew. Chem. Int. Ed.* **2005**, *44*, 7922-7925.

77. Kang, H.; Facchetti, A.; Zhu, P.; Jiang, H.; Cariati, E.; Righetto, S.; Ugo, R.; Zuccaccia, C.; Macchioni, A.; Stern, C. L.; Liu, Z.; Ho, S.-T.; Brown, E. C.; Ratner, M. A.; Marks, T. J. *J. Am. Chem. Soc.* **2007**, *129*, 3267-3286.

78. He, G. S.; Zhu, J.; Baev, A.; Samoc, M.; Frattarelli, D. L.; Watanabe, N.; Facchetti, A.; Agren, H.; Marks, T. J.; Prasad, P. N. *J. Am. Chem. Soc.* **2011**, *133*, 6675-6680.

79. Shi, Y.; Lou, A. J.-T.; He, G. S.; Baev, A.; Swihart, M. T.; Prasad, P. N.; Marks, T. J. *J. Am. Chem. Soc.* **2015**, *137*, 4622-4625.

80. Boeglin, A.; Barsella, A.; Chaumeil, H.; Ay, E.; Rotzler, J.; Mayor, M.; Fort, A.; *Proc. of SPIE* **2010**, *7774*, 777408.

81. Wilson, T. M.; Ricks, A. B.; Scott, A. M.; Ratner, M. A.; Wasielewski, M. R. *J. Phys. Chem. A* **2008**, *112*, 4194-4201.

82. Colvin, M. T.; Ricks, A. B.; Scott, A. M.; Co, D. T.; Wasielewski, M. R. *J. Phys. Chem. A* **2012**, *116*, 1923-1930.

83. Hoshino, M.; Uekusa, H.; Tomita, A.; Koshihara, S.; Sato, T.; Nozawa, S.; Adachi, S.; Ohkubo, K.; Kotani, H.; Fukuzumi, S. *J. Am. Chem. Soc.* **2012**, *134*, 4569-4572.

84. Fukuzumi, S.; Ohkubo, K. *Org. Biomol. Chem.* **2014**, *12*, 6059-6071.

85. Bao, C.; Zhu, L.; Lin, Q.; Tian, H. *Adv. Mater.* **2015**, *27*, 1647-1662.

86. Harabuchi, Y.; Taketsugu, T.; Maeda, S. *Phys. Chem. Chem. Phys.* **2015**, *17*, 22561-22565.

General Conclusion

1. Molecular Geometries that Induce Fluorescence Functionality

2. Another Aspect of Chapter 4 and its Perspective; Engineering of a Conical Intersection

3. Comments about the Position of **BDAA**s in Studies of Solid-State Fluorescence; the Intersection where Solid-State Photophysics Meets Synthetic Organic Chemistry

4. References

1. Molecular geometries that induce fluorescence functionality

Table 1. The summary of "Functional geometry" that induce fluorescence functionality and their underlying mechanism.

Geometry	Function	Involving State-interactions
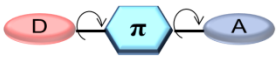 Torsion at D-A junctions	Controlled Solvatochromism Aggregation-induced emission Dual-mode fluorescence	^1L_a-^{1}CT mixing ^1L_b-^{1}CT interconversion
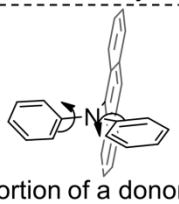 Distortion of a donor plane	Extension of π-conjugation	^1L_a-^{1}CT mixing
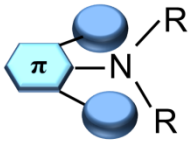 Highly twisted *N*,*N*-dialkylamines	Aggregation-induced emission Viscosity-sensitive fluorescence	S_1/S_0 conical intersection
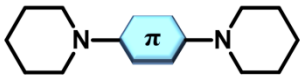 Confronting piperidyl groups	Chemo-selective quenching and photodegradation	Electronic repulsions through ^1L_a-^{1}CT mixing

In this thesis, various fluorescence functions were derived from classic aromatic hydrocarbons such as biphenyl, anthracene, naphthalene and pyrene. The core strategy that was adopted in this thesis was "molecular geometry"; particular structural parameters which govern electronic structures of π-conjugated systems were utilized to realize superior fluorescence and photochemical functions.

In Chapter 2, it was torsion at donor-acceptor (D−A) junctions that controlled fluorescence solvatochromism of biphenyl analogues of PRODAN, and bring about aggregation-induced emission and dual-mode fluorescence to the binaphthyl. Chapter 3 demonstrated that π-conjugation could be extended also by distortion of a donor plane. Both torsion at D−A junctions and distortion of a donor plane manipulated extents and balances on ^1L_a–^{1}CT mixing. Correlation between ^1L_a–^{1}CT mixing and torsion at D−A junctions has already been elucidated in theoretical and spectroscopic investigations of TICT phenomena.[1] Nevertheless, this thesis first demonstrated that excited-state polarization and fluorescence solvatochromism could be finely tuned by imposing steric

restrictions. As exemplified by Thioflabin-T,[2] a fluorescent probe with a chemical structure that could selectively bind to a particular biomolecule has produced a breakthrough in molecular biology and therefore a chemical structure of a solvatochromic dye should be determined by compatibility toward a target molecule. Taking the fact into account, the control of solvatochromism by torsion deserves a "trump card" on the design of fluorescent probe because my strategy does not require any major modification of a chromophore and a functional group.

Chapter 4 revealed strongly twisted *N*,*N*-dialkylamines to activate drastic aggregation-induced emission and viscosity-sensitive fluorescence of naphthalene, anthracene and pyrene. Structural simplicity of these *N*,*N*-dialkylaminoarenes is unprecedented among reported AIEgens and fluorescent molecular rotors. Strong solid-state fluorescence, acute S/N ratio, colour tuning by means of regioisomerism, and large stokes shift of **9,10-BPA**, **1,4-BPA**, and **DMe-BDAN** are suitable to various applications. For example, **9,10-BPA** and **1,4-BPA** should be promising probe for super-resolution imaging such as multicolour-STED (stimulated emission depletion) techniques.[3] Since the facile procedure for terminal functionalization of **9,10-BDAA** and **DMe-BDAN** was presented in Chapter 5, these fluorophore now become available for these practical applications.

Chapter 6 demonstrated that the molecular-geometry approach is promising strategy not only for fluorescence functionality but also for photochemical functionality. Though photodegradation reaction of **1,4-BPN**-based cross-linker is not as clean as those based on *o*-nitrobenzyl groups, structural simplicity, facile preparation, fluorescence sensing, and chemo-selective photodegradation of the cross-linker are sufficient to motivate material scientists to employ **1,4-BPN**–based cross-linker for design of functional materials.

2. Another aspect of Chapter 4 and its perspective; engineering of a conical intersection

Chapter 4 is also important from the standpoint of basic science because it is the first example that succeeded in "engineering" of S_1/S_0 conical intersection of aromatic hydrocarbons. Internal conversion is one of the most well-known photophysical process

as well as intersystem crossing. Nevertheless, it is still difficult to control which vibrational mode plays the principal role in internal conversion processes whereas intersystem crossing can easily be controlled by introduction of bromo- or iodo-group (heavy-atom effect),[4] carbonyl group (El-Sayed rule),[5] and severe torsion at D-A junction (minimizing ^{1}CT-^{3}CT gap).[6] Stabilization of S_1/S_0 conical intersection (CI) is an answer for how to have an excited wave packet undergo efficient internal conversion with a low-frequency, large-amplitude mode. Though S_1/S_0 CI of benzene is also well-known as "Channel 3",[7] no one has not attempted to stabilize it by any chemical modification and no one utilized it to derive any photophysical functionality. By deriving drastic AIE and viscosity-sensitive fluorescence through stabilization of S_1/S_0 CI, this thesis underscored the importance of a **thermally inaccessible** S_1/S_0 CI as well as a thermally accessible one. Therefore, the thesis is also to inspire theoretical chemists to explore S_1/S_0 CI of broader range of chromophores. At the same time, dewar-benzene like S_1/S_0 CI should be interesting from the standpoint of ultrafast spectroscopy. Recent spectroscopic techniques could identify what vibration mode guided a wave packet toward S_1/S_0 CI even of a **photophysical process** (e.g. charge recombination of the TCNQ-TMB complex)[8] as well as a photochemical process (e.g. the primary isomerization of rhodopsin).[9] Such a state-of-the-art spectroscopic technique may be able to analyse S_1/S_0 CI of **9,10-BDAA**.

3. Comments about the position of BDAAs in studies of solid-state fluorescence; the intersection where solid-state photophysics meets synthetic organic chemistry

Recently, design of organic dyes with strong solid-state fluorescence has become the attractive subject for many researchers, especially those who are specialized in synthetic organic chemistry and material chemistry.[10-11] Since their main interests are in practical aspects, their design strategy predominantly focuses upon how to avoid "detrimental" so-called π-π interactions with adjacent chromophores. Therefore, various synthetic strategy has been adopted to make each chromophore spatially apart from neighbouring one. In the disparate context, enormous efforts have been devoted to understand photophysics of molecular crystals.[12-18] They scrutinized how do dye

molecules interact with each other in solid states rather than avoiding it. The scope of interactions that the photophysics of molecular crystals covered was far beyond interactions discussed in the recent context of synthetic chemistry and material chemistry. Especially theoretical and experimental studies about exciton-phonon (or vibration) coupling[16-18] was not discussed by these synthetic chemists but extremely important on the design of highly solid-state fluorescent organic dyes. Some experimental and theoretical studies revealed that when exciton-phonon coupling got strong under e.g. applying pressure,[18] local lattice deformation sometimes trapped delocalized exciton into a particular site, resulting in fluorescent "self-trapped exciton". Unfortunately, design and synthesis were out of scope of these photophysical studies and therefore the concept of local lattice deformation has not been employed so far on the design of solid-state fluorescent organic dyes.

This thesis is about design and syntheses, but at the same time, focuses upon structural relaxation after photoexcitation. As elucidated in Chapter 4-1 and 4-2, **1,4-BPA**, **9,10-BPA** and its alkyl analogues features extremely large stokes shifts with minimal structural deformations. Furthermore, solid-state fluorescence spectra of **1,4-BPA** and **9,10-BPA** were almost identical with those measured in toluene solution, indicating excitons of **1,4-BPA** and **9,10-BPA** were monomeric even in solid states. When "local lattice deformation" was rephrased as "structural relaxation after photoexcitation", the theory of self-trapped exciton[17-18] could explain strong monomeric fluorescence of **1,4-BPA** and **9,10-BPA**. Regardless of their crystal structures, distances between neighbouring chromophores, existence of impurities, excitons of **1,4-BPA** and **9,10-BPA** should be trapped to monomeric state unless other states become lower-lying than the relaxed S_1 state of an individual molecule. Therefore **1,4-BPA**, **9,10-BPA** and its alkyl analogues can be regarded to be striking example of self-trapped excitons though their "local lattice deformation" is designed focusing on intramolecular structural relaxations (i.e. Aryl-N rotation for **1,4-BPA** and planarization of the *N*,*N*-dialkylamine planes for **9,10-BPA** and its alkyl analogues). Similarly, there should be myriad of possible designs when one notices that the term "phonon" includes intramolecular vibration and the term "lattice" can be associated with a conformation of an individual molecule.

Importance of local structures in bulk materials is not limited to molecular systems. Recently inorganic chalcogenides are in spotlight of solid-state physics and chemistry due to its strong electronic interaction between adjacent sites. However, electronic interactions within their sites has been focused much less than inter-site interactions. As well-known in the chemistry of transition metal complexes, electronic structures of d-electron systems are extremely sensitive to their molecular geometries. The fact implies that slight structural deformations of local structure (e.g. by replacing an anion with larger one) drastically changes an electronic nature of each site in strongly-correlated electron systems, resulting in great variation in inter-site interactions and unexpected phenomena. For instance, Jahn-Teller distorsion originates from interactions between degenerated or proximate electronic configurations. Conversely, their interactions (or mixing) between different electronic configurations could be controlled by imposing steric restrictions along a reaction coordinate of Jahn-Teller distorsion. Such a modification of electronic state may end up minor effects in the level of an individual metal complex but what happens if two different electronic states are balanced at each site of strongly correlated systems? Therefore, correlation between "molecular (or local) structure" and its electronic structure should be an attractive topic no matter whether an material consists of organic molecules or not.

4. References

1. Grabowski, Z. R.; Rotkiewicz, K.; Rettig, W. *Chem. Rev.* **2003**, *103*, 3899-4032.
2. Amdursky, N.; Erez, Y.; Huppert, D. *Acc. Chem. Res.* **2012**, *45*, 1548-1557.
3. Göttfert, F.; Wurm, C. A.; Mueller, V.; Berning, S.; Cordes, V. C.; Honigmann, A.; Hell, S. W. *Biophys. J.* **2013**, *105*, L01.
4. Khudyakov, I. V.; Serebrennikov, Y. A.; Turro, N. J. *Chem. Rev.* **1993**, *93*, 537-570.
5. El-Sayed, M. A. *Acc. Chem. Res.* **1968**, *1*, 8-16.
6. Sato, K.; Shizu, K.; Yoshimura, A.; Miyazaki, H.; Adachi, C. *Phys. Rev. Lett.* **2013**, *110*, 247401.
7. Li, Q.; Tapia, D. M.; Paterson, M. J.; Migani, A.; Bearpark, M. J.; Robb, M. A.; Blancafort, L. *Chem. Phys.* **2010**, *377*, 60-65.
8. Hoffman, D. P.; Ellis, S. R.; Mathies, R. A. *J. Phys. Chem. A* **2014**, *118*, 4955-4965.

9. Kukura, P.; McCamant, D. W.; Yoon, S.; Wandschneider, D. B.; Mathies, R. A. *Science* **2005**, *310*, 1006-1009.
10. Mei, J.; Leung, N. L. C.; Kwok, R. T. K.; Lam, J. W. Y.; Tang, B. Z. *Chem. Rev.* **2015**, *115*, 11718-11940.
11. Shimizu, M.; Hiyama, T. *Chem. Asian J.* **2010**, *5*, 1516-1531.
12. Davydov, A. S. *Usp. Fiz. Nauk* **1964**, *82*, 393-448.
13. Colson, S. D.; Hanson, D. M.; Kopelman, R.; Robinson, G. W. *J. Chem. Phys.* **1968**, *48*, 2215-2230.
14. Silbey, R.; Jortner, J.; Rice, S. A. *J. Chem. Phys.* **1965**, *42*, 1515-1534.
15. Yamagata, H.; Norton, J.; Hontz, E.; Olivier, Y.; beljonne, D.; Bredas, J. L.; Silbey, R. J.; Spano, F. C. *J. Chem. Phys.* **2011**, *134*, 204703.
16. Levinson, Y. B.; Rashba, E. I. *Rep. Prog. Phys.* **1973**, *36*, 1499-1565.
17. Toyozawa, Y. *J. Phys. Soc. Jpn.* **1989**, *58*, 2626-2629.
18. Mizuno, K.; Furukawa, M.; Matsui, A. *J. Phys. Soc. Jpn.* **1991**, *60*, 2768-2777.